

Zeroth-Order Regularized Optimization (ZORO): Approximately Sparse Gradients and Adaptive Sampling

HanQin Cai¹, Daniel Mckenzie¹, Wotao Yin^{2,1}, and Zhenliang Zhang²

¹Department of Mathematics,
University of California, Los Angeles,
Los Angeles, CA, USA.

²Damo Academy,
Alibaba US,
Seattle, WA, USA.

November 19, 2021

Abstract

We consider the problem of minimizing a high-dimensional objective function, which may include a regularization term, using only (possibly noisy) evaluations of the function. Such optimization is also called derivative-free, zeroth-order, or black-box optimization. We propose a new **Z**eroth-**O**rd^er **R**egularized **O**ptimization method, dubbed ZORO. When the underlying gradient is approximately sparse at an iterate, ZORO needs very few objective function evaluations to obtain a new iterate that decreases the objective function. We achieve this with an adaptive, randomized gradient estimator, followed by an inexact proximal-gradient scheme. Under a novel approximately sparse gradient assumption and various different convex settings, we show the (theoretical and empirical) convergence rate of ZORO is only logarithmically dependent on the problem dimension. Numerical experiments show that ZORO outperforms the existing methods with similar assumptions, on both synthetic and real datasets.

1 Introduction

Zeroth-order optimization, also known as derivative-free or black-box optimization, appears in a wide range of applications where either the objective function is implicit or its gradient is impossible or too expensive to compute. These applications include structured prediction [1], reinforcement learning [2], bandit optimization [3, 4] optimal setting search in material science experiments [5], adversarial attacks on neural networks [6, 7], and hyper-parameter tuning [8].

Email addresses: hqcai@math.ucla.edu (H.Q. Cai), mckenzie@math.ucla.edu (D. Mckenzie), wotao.yin@alibaba-inc.com (W. Yin), and zhenliang.zhang@alibaba-inc.com (Z. Zhang).

In this work, we propose a new method, which we coin ZORO, for high dimensional *regularized* zeroth-order optimization problems:

$$\underset{x \in \mathbb{R}^d}{\text{minimize}} F(x) := f(x) + r(x), \quad (1)$$

where $r(x)$ is an *explicit* proximable function that enforces constraints and encodes the solution’s structure, and $f(x)$ is accessible only through a noisy zeroth order *oracle*:

$$E_f(x) = f(x) + \xi, \quad (2)$$

where ξ is the unknown oracle noise. When we call the oracle with an input x , it returns $E_f(x)$ in which ξ may or may not change every time.

The complexities of zeroth-order methods are measured in the number of oracle queries needed to achieve a target accuracy. ZORO reduces such complexities by exploiting the fact that most gradients (*i.e.*, those in the set $\{\nabla f(x) : x \in \mathbb{R}^d\}$) are often compressible, meaning that the sorted sizes of their components decay like a polynomial! In Figure 1, we can see the quick decays of the sorted gradient’s components by magnitude and how consistent they are. To generate the figure, we sampled gradients at 100 random points in each of the two real examples (see the numerical section.) In certain examples, gradients at some points can even be sparse, *i.e.*, many components being exactly zero. Exploiting gradient compressibility is important but largely unexplored in the community that uses oracle queries to estimate the gradient and then apply a gradient-based method. Seminal works in this community include [9, 10, 11]; generally speaking, gradient estimation based methods work well with convex objective functions [12, 13, 14], but are also suitable with some non-convex models [11, 15] and may allow parallel optimization [16, 17]. However, all these methods suffer a mild curse of dimensionality as their complexities depend at least linearly on d . (In contrast, the oracle complexities of first-order gradient methods are independent of d .) This has limited to the applications of those zeroth order methods to relatively low dimensions. Not that they cannot be attempted on high dimensions, but the number of oracle calls can be unbearably large. In contrast, when the gradients are compressible, ZORO will improve the dependence to $O(\log d)$, a drastic reduction from $O(d)$.

Exact sparsity of gradients has been recently exploited in the pioneering works [14] and [18]. Their methods already enjoy a query complexity that is polynomially dependent on $\log(d)$. They assume everywhere exact sparsity, but it is unclear how many C^1 functions can be exactly sparse everywhere.

Compressibility is a more practical assumption than sparsity. To clarify, compressible gradients can be completely dense. For example, in hyper-parameter tuning, the performance is often sensitive to only a few hyper-parameters, so they tend to carry more significant weights in gradients. But, less-sensitive ones still need to be tuned. So, good methods need to explore the opportunity offered by compressible gradients when they are present and still work even when gradients are not sparse.

ZORO employs an *adaptive sampling* strategy for improved gradient estimation. When all but finitely many gradients are compressible, ZORO’s oracle complexity is $O(\log d)$ and, otherwise, $O(d)$. There is no penalty for exploiting compressibility when the gradients are not compressible. Nonetheless, in the examples we have tested, compressibility is always present and leads to significant speedup.

ZORO works with both noise-free oracles (*i.e.*, $\xi = 0$ in (2)) and *adversarially noisy* oracles. Adversarial noises arise when the oracle calls are simplified for faster speed (*e.g.*, a simulation that is early terminated) or when the noise has non-stationary distributions. In both cases, it is difficult

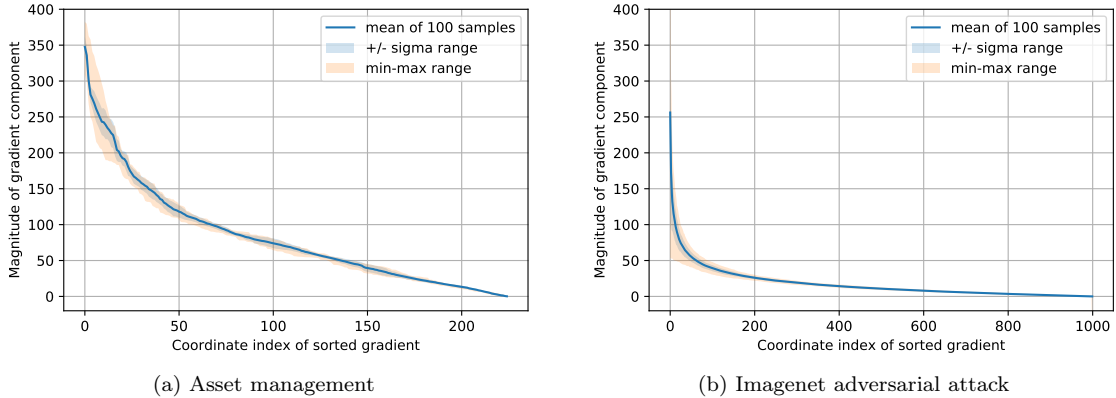


Figure 1: Sorted gradient components at 100 random points in two optimization problems.

to know the noise distributions, so it is best to treat them as adversaries. To clarify, ZORO should work with Gaussian noise without modification, but for space reasons, only adversarial noise is analyzed.

We include a regularization term r since they are frequently useful in modeling. Typical examples include non-negativity constraints $x \geq 0$, box constraints $\ell \leq x \leq u$, and solution sparsity $\|x\|_1 \leq s$. The fact that f is available only through an oracle should not prevent us from using prior knowledge explicitly. ZORO applies the proximal mapping of r while accessing f only through its zeroth order oracle.

ZORO’s main iteration is based on the proximal-gradient method but uses an approximate gradient $\hat{\mathbf{g}}_k$ that is estimated from multiple (noisy) samples of f near x_k . The estimation uses randomized finite differences and compressed sensing. But, the process is trickier than simply combining proximal-gradient, finite difference, and compressed sensing. Very carefully, we have to control the gradient error, that is, the difference between $\hat{\mathbf{g}}_k$ and $\mathbf{g}_k = \nabla f(x_k)$. The error has three contributing sources: the noise of the oracle, the error due to finite differencing, and the error introduced by compressed sensing. The latter two can be controlled, but not eliminated, by setting proper sampling radii and numbers of samples, respectively. We manage to characterize how those errors affect convergence speed and final solution accuracy. Also, if the oracle’s adversarial noise is bounded, ZORO converges to a solution neighborhood; if the oracle is noise-free, then ZORO can converge to an exact solution asymptotically despite the existence of the finite-differencing and compressed-sensing errors.

In this paper, we show ZORO has sublinear convergence for smooth convex f and smooth nonconvex f . The results of exact convergence under noise-free oracle (but the presence of other two kinds of noise) require a new line of analysis for the proximal-gradient method. Including both a regularization term and noise takes us to a partially uncharted area of analyzing noisy proximal-gradient descent, which we overcome with novel analysis. In particular, we prove sequence boundedness instead of assuming them.

1.1 Review of query complexity

Arguably, the first methods to employ zeroth order gradient estimators within a gradient-based optimization method are FDSA [9] and SPSA [10]. SPSA was analyzed in [11]¹ to have, after T oracle queries, $f(x_T) - \min f \leq O(d/T)$ for noise-free oracles, and $\mathbb{E}[f(x_T) - \min f] \leq O(d/\sqrt{T})$ for stochastic oracles under: $E_f(x) = F(x, \xi)$, but satisfying $\mathbb{E}[F(x, \xi)] = f(x)$. This convergence rate was improved to $O(\sqrt{d/T})$ in [15], and this rate is also achieved in [16]. In [20], it is shown that for strongly convex $f(x)$ and oracle of the form (2) with zero-mean noise, the zeroth order optimization problem is in $\Omega(\sqrt{d/T})$. Thus, the rate achieved in [15, 16] is essentially optimal without placing further assumptions on $f(x)$. As we have mentioned, [14] proposed the exact sparse gradient assumption, $\|\nabla f(x)\|_0 \leq s$ for all x , and, using a mirror descent scheme and assuming zero-mean oracle noise, obtained $O((s/T)^{1/3} \log(d))$. [18] also used the sparse gradient assumption but projected gradient descent with carefully chosen step sizes to achieve $O((s/T)^{1/2} \log(d))$. However, their analysis implicitly requires that the support of $\nabla f(x)$ is *fixed*, which is a very stringent requirement. Finally, for a comprehensive overview of zeroth-order optimization methods, we refer the interested readers to the recent survey article [21].

1.2 Notation

For any vector or matrix, $\|\cdot\|_0$ counts the non-zero entries, while $\|\cdot\|_1$ is the entry-wise ℓ_1 norm. We shall frequently use $\mathbf{g} := \nabla f(x)$ when the point x in question is clear. We also write $\min F := \min\{F(x) : x \in \mathbb{R}^d\}$ and $e_k := F(x_k) - \min F$, where x_k is the k th iterate. Moreover, $[x]_{(s)}$ denotes the best s -sparse approximation to vector x while $|x|_{(i)}$ denotes the i th largest-in-magnitude component of x .

1.3 Assumptions

We present a series of assumptions used in this paper.

Assumption 1 (Sparse/compressible gradients). We consider two different types for the gradients: The gradients of f are *s-sparse* if $\|\nabla f(x)\|_0 \leq s_{\text{exact}}$ for all $x \in \mathbb{R}^d$; The gradients of f are *compressible* if there exists a $p \in (0, 1)$ such that $|\nabla f(x)|_{(i)} \leq i^{-1/p} \|\nabla f(x)\|_2$.

Compressibility does not explicitly specify support size s , but it implies

$$\|\nabla f(x) - [\nabla f(x)]_{(s)}\|_1 \leq (1/p - 1)^{-1} \|\nabla f(x)\|_2 s^{1-1/p} \quad (3)$$

$$\|\nabla f(x) - [\nabla f(x)]_{(s)}\|_2 \leq (2/p - 1)^{-1/2} \|\nabla f(x)\|_2 s^{1/2-1/p}; \quad (4)$$

see, for example, [22, Section 2.5]. The next assumption is needed *only* when the oracle is noisy.

Assumption 2 (Bounded Hessian (optional assumption)). Let f be twice differentiable. Then there exists a constant H such that $\|\nabla^2 f(x)\|_1 \leq H$ for all $x \in \mathbb{R}^d$.

Next, we present a standard assumption on the existence of minimizer of F and the smoothness of f .

¹This later appeared as [19].

Algorithm 1 Zeroth Order Regularized Optimization Method (ZORO)

- 1: **Input:** x_0 : initial point; s : gradient sparsity level; α : step size; β : query radius parameter; δ_0 : initial query radius, ϕ (*optional*): error tolerance for OppGradEst.
 - 2: $m \leftarrow b_1 s \log(d/s)$ where b_1 is as in Lemma B.2. Typically $b_1 \approx 4$ is appropriate
 - 3: **for** $i = 1$ **to** m **do**
 - 4: Generate Rademacher random vector z_i .
 - 5: **end for**
 - 6: **for** $k = 0$ **to** K **do**
 - 7: $\hat{\mathbf{g}}_k \leftarrow$ Gradient Estimation($x_k, s, \delta_k, \{z_i\}_{i=1}^m$) (see Alg. 3) or,
 $(\hat{\mathbf{g}}_k, \{z_i\}_{i=1}^m) \leftarrow$ OppGradEst($x_k, \hat{S}_{k-1}, \delta_k, \{z_i\}_{i=1}^m, \phi$) (see Alg. 4 in Appendix)
 - 8: $x_{k+1} \leftarrow \mathbf{prox}_{\alpha r}(x_k - \alpha \hat{\mathbf{g}}_k)$
 - 9: $\delta_{k+1} \leftarrow \begin{cases} \beta \|\hat{\mathbf{g}}_k\|_2 & \text{Noise-free oracle case and } r(x) = 0 \\ 1/k^{1.1} & \text{Noise-free oracle and } r(x) \neq 0 \\ \sqrt{2\sigma/H} & \text{Noisy oracle case} \end{cases}$
 - 10: $\hat{S}_k \leftarrow \text{supp}(\hat{\mathbf{g}}_k)$
 - 11: **end for**
 - 12: **Output:** x_K : minimizer of (1).
-

Assumption 3 (Solution existence and Lipschitz gradients). (i) The solution set of F is non-empty. (ii) For any $x, y \in \mathbb{R}^d$, we have that $\|\nabla f(x) - \nabla f(y)\|_2 \leq L\|x - y\|_2$ for some constant L .

Note that we are not assuming that we have access to ∇f , only that the Lipschitz property holds.

Assumption 4 (Adversarially noisy oracle). The oracle noise ξ is bounded: $\|\xi\|_2 \leq \sigma$.

Our analyses considers different settings of regularized objective function F , involving convex and non-convex components. We provide the standard definitions of convexity, coercivity, and an extended notion of proximal operator in Appendix A.

2 Proposed method

ZORO is based on the iteration:

$$x_{k+1} = \mathbf{prox}_{\alpha r}(x_k - \alpha \hat{\mathbf{g}}_k), \quad k = 0, 1, \dots,$$

where $\hat{\mathbf{g}}_k$ is a noisy gradient estimator that we derive below. ZORO is given in Algorithm 1.

2.1 Gradient estimation

Choose a query number m and a sampling radius δ , and let $\{z_i\}_{i=1}^m \in \mathbb{R}^d$ be Rademacher random vectors, that is, $(z_i)_j = \pm 1$ with equal probability for all $i = 1, \dots, m$ and $j = 1, \dots, d$. (Gaussian and certain other types of random vectors will work, too. For space reasons, we investigate only the Rademacher type.) To construct each measurement (in the compressed sensing sense) we make

two oracle queries, at x and at $x + \delta z_i$, and compute the (noisy) finite difference (divided by \sqrt{m}) along direction z_i :

$$y_i = \frac{1}{\sqrt{m}} \frac{E_f(x + \delta z_i) - E_f(x)}{\delta}. \quad (5)$$

We present this procedure as Algorithm 2. We can write $y_i = \frac{1}{\sqrt{m}} z_i^\top \mathbf{g} + \text{noise}$; see Lemma B.1.

Since $\nabla f(x)$ is compressible, we approximate its gradient as

$$\hat{\mathbf{g}} = \operatorname{argmin}_{\mathbf{v} \in \mathbb{R}^d} \|Z\mathbf{v} - \mathbf{y}\|_2 \quad \text{such that } \|\mathbf{v}\|_0 \leq s, \quad (6)$$

where $\mathbf{y} = [y_1, \dots, y_m]^\top$ and $Z \in \mathbb{R}^{m \times d}$ is the *sensing matrix* whose i -th row is $\frac{1}{\sqrt{m}} z_i^\top$. We propose to solve Problem (6) approximately using CoSaMP [22], and present the resulting gradient estimation procedure as Algorithm 3. Let us mention that we could use LASSO, which is similar to the approach taken in [14]. However, there are at least three reasons why CoSaMP could be preferable: (i) The LASSO estimator is typically biased [23], while the CoSaMP estimator does not have this problem. This makes CoSaMP more appropriate for the compressible gradients case; (ii) CoSaMP is faster for small sparsity levels, s , which are sufficient to get a descent (see Figures 5 and 6 in Appendix E for numerical comparison); (iii) Tuning LASSO's parameter λ is indirect thus difficult when it comes to ensuring convergence.

The next two theorems relate the quality of the estimated gradient $\hat{\mathbf{g}}_k$ to \mathbf{g}_k and parameters. We introduce

$$\psi = \psi(s) := \begin{cases} 0 & \text{if } \nabla f(x) \text{ is } s\text{-sparse,} \\ Cs^{1/2-1/p} & \text{if } \nabla f(x) \text{ is compressible.} \end{cases}$$

to quantify the error attributable to the tail of $\|\mathbf{g}_k\|$ in the compressible case. Note that C , defined in Lemma B.6, depends on p and $\{z_i\}_{i=1}^m$ but not on s .

Theorem 2.1. *Suppose that $\nabla f(x)$ is s -sparse; but if $\nabla f(x)$ is compressible then let s be chosen large enough such that $\psi < \min \left\{ \frac{1-\alpha L}{2-\alpha L}, \frac{2-\alpha L}{4-\alpha L} \right\}$. Suppose further that $f(x)$ satisfies Assumption 3 and that $\alpha < 1/L$. Choose ε_{rel} and n such that:*

$$\psi + \rho^n < \varepsilon_{\text{rel}} < \min \left\{ \frac{1 - \alpha L}{2 - \alpha L}, \frac{2 - \alpha L}{4 - \alpha L} \right\},$$

and define:

$$\beta = \frac{2(\varepsilon_{\text{rel}} - \psi - \rho^n)(1 - \alpha L - \varepsilon_{\text{rel}}(2 - \alpha L))}{\tau H(1 - \varepsilon_{\text{rel}})}.$$

If $\|\mathbf{g}_0 - \hat{\mathbf{g}}_0\|_2 \leq \varepsilon_{\text{rel}} \|\mathbf{g}_0\|_2$ and $\delta_k < \beta \|\hat{\mathbf{g}}_{k-1}\|_2$, then:

$$\|\mathbf{g}_k - \hat{\mathbf{g}}_k\|_2 \leq \varepsilon_{\text{rel}} \|\mathbf{g}_k\|_2$$

for all k with probability $1 - (s/d)^{b_2 s}$ where b_2 is defined as in Lemma B.2.

The exact values of ρ and τ are given in [24]. The constants b_1 and b_2 are defined in Lemma B.2. Note that as $p \in (0, 1)$ we can make ψ (almost) arbitrarily small by taking s to be larger.

Theorem 2.2. *Suppose that $\nabla f(x)$ is s -sparse and $f(x)$ satisfies Assumptions 2 and 3, $\delta_k = \delta = \sqrt{2\sigma/H}$ and n is sufficiently large. Then for all k :*

$$\|\hat{\mathbf{g}}_k - \mathbf{g}_k\|_2 \leq 2\sqrt{2\tau\sigma H}$$

with probability at least $1 - (s/d)^{b_2 s}$.

Algorithm 2 Sample (used by Alg. 3 and Alg. 4)

- 1: **Input:** x : current point; δ : query radius; r , $\{z_i\}_{i=1}^r$: sample number and directions.
 - 2: Sample at point x , obtain $E_f(x)$.
 - 3: **for** $i = 1$ **to** r **do**
 - 4: Sample at point $x + \delta z_i$ to obtain $E_f(x + \delta z_i)$.
 - 5: $y_i \leftarrow (E_f(x + \delta z_i) - E_f(x))/\delta$
 - 6: **end for**
 - 7: $\mathbf{y} \leftarrow [y_1, \dots, y_r]^\top$
 - 8: **Output:** \mathbf{y}
-

Algorithm 3 Gradient Estimation

- 1: **Input:** x : current point; s : sparsity level; δ : query radius; $\{z_i\}_{i=1}^m$: sample directions.
 - 2: $\mathbf{y} \leftarrow \frac{1}{\sqrt{m}} \text{Sample}(x, \delta, \{z_i\}_{i=1}^m)$ (see Alg. 2)
 - 3: $Z \leftarrow \frac{1}{\sqrt{m}} [z_1, \dots, z_m]^\top$
 - 4: $\hat{\mathbf{g}} \approx \text{argmin}_{\|\mathbf{g}\|_0 \leq s} \|Z\mathbf{g} - \mathbf{y}\|_2$ by CoSaMP
 - 5: **Output:** $\hat{\mathbf{g}}$
-

In Appendix D we quantify precisely how large n should be.

2.2 Relative-error gradient descent

Given the above bounds on $\|\mathbf{g}_k - \hat{\mathbf{g}}_k\|_2$, proving that ZORO converges is largely a matter of adapting existing results on inexact (proximal) gradient descent. We provide these in Appendix. We highlight that one novel difficulty we overcame was the issue of convergence given a *relative bound* on $\|\mathbf{g}_k - \hat{\mathbf{g}}_k\|_2$:

Theorem 2.3 (Sublinear convergence with relative errors). *Suppose that $f(x)$ is convex, $r(x) = 0$, Assumption 3 holds. Suppose further that $\|\mathbf{g}_k - \hat{\mathbf{g}}_k\|_2 \leq \varepsilon_{\text{rel}} \|\mathbf{g}_k\|_2$, $\alpha < 2/L$ and $\|x_k - P_*(x_k)\|_2 \leq R$ for all k , then:*

$$e_k \leq \frac{e_0}{ke_0/(c_9 R^2) + 1} \sim c_9 R^2 \cdot \frac{1}{k}.$$

The constants c_7 , c_8 and c_9 are defined as in Lemma C.6.

We remark that the assumption $\|x_k - P_*(x_k)\|_2 \leq R$ is rather strong. In Proposition C.7 we provide weaker sufficient conditions under which this holds.

2.3 Opportunistic Sampling

It would be nice for Algorithm 3 to work without assuming gradient compressibility, but still be able to exploit this when it arises. Moreover, the support of the previous gradient estimate is important information that should not be ignored. We present an algorithm incorporating these observations as Algorithm 4 in Appendix B. Informally, Algorithm 4 proceeds as:

- (i) Take only s samples and solve a least squares problem with support restricted to $\text{supp}(\mathbf{g}_{k-1})$. If the relative error in this solution is small, return it immediately as $\hat{\mathbf{g}}_k$.

- (ii) Otherwise, run a variation of Gradient Estimation (lines 8–10 of Algorithm 4) to reuse the s samples we have already taken. Check whether the solution is sufficiently accurate (line 12).
- (iii) Until a sufficiently accurate solution is found, we take oracle queries while retaining our earlier samples; estimate the gradient from these samples, old and new (lines 13–18 of Algorithm 4).

At worst, we make around d queries, no worse than the dense gradient estimators. Our tests never needed this many though. For example, in the asset allocation experiment below, each gradient has 225 entries, but ZORO can converge with approximate gradients with only 40 to 72 nonzeros.

3 Query complexity

Given the tools of Section 2, it is possible to prove rates of convergence for ZORO in a variety of cases. Here we present results for three, representative, scenarios.

Theorem 3.1. *Suppose that $f(x)$ is convex and coercive, that $r(x) = 0$ and that the oracle is noise-free ($\sigma = 0$). Assume the hypotheses of Theorem 2.1. Let $r(x) = 0$ and let x_K be the iterate returned by ZORO after making T oracle queries, where $K = T/m$. Then:*

$$e_K \leq \frac{c_9 e_0 R^2}{T e_0 / b_1 s \log(d/s) + c_9 R^2} = O\left(\frac{s \log(d/s)}{T}\right),$$

with probability at least $1 - (s/d)^{b_2 s}$.

The next two results allow for oracle noise.

Corollary 3.2. *Assume the hypotheses of Theorem 2.2. Assume, in addition that $f(x)$ and $r(x)$ are convex, that $F(x)$ is coercive and $\|\partial F(x)\|_2$ is coercive with respect to $f(x)$. Let x_K be the iterate returned by ZORO with $\alpha < 2/L$ after making T oracle queries, where $K = T/m$. Then:*

$$e_K \leq \max\left\{\frac{c_7 e_0 R^2}{T e_0 / b_1 s \log(d/s) + 2c_7 R^2}, 2^{\frac{3}{4}} R c_8^{\frac{1}{2}} (\tau \sigma H)^{\frac{1}{4}}\right\} = O\left(\max\left\{\frac{s \log(d/s)}{T}, R(\sigma H)^{\frac{1}{4}}\right\}\right).$$

with probability $1 - (s/d)^{b_2 s}$.

The constants b_1 and b_2 are defined as in Lemma B.2. We remark that the coercivity assumptions are necessary. Consider the following simple, one-dimensional, example. Let $f(x)$ be the Huber loss function:

$$f(x) = \begin{cases} \frac{1}{2}x^2 & \text{for } |x| \leq m \\ m(|x| - \frac{1}{2}m) & \text{otherwise} \end{cases}$$

while $r(x) = 0$ and $\sigma > m^2$. From Theorem 2.2 we get that, at worst:

$$\|\mathbf{g}_k - \hat{\mathbf{g}}_k\| \approx 2^{3/2} \tau^{1/2} m > 2m \geq 2\|\mathbf{g}_k\| \quad (\text{as } H = 1).$$

That is, for all k the noise can be chosen adversarially such that $\text{sign}(\hat{\mathbf{g}}_k) \neq \text{sign}(\mathbf{g}_k)$, hence the inexact gradient descent may diverge.

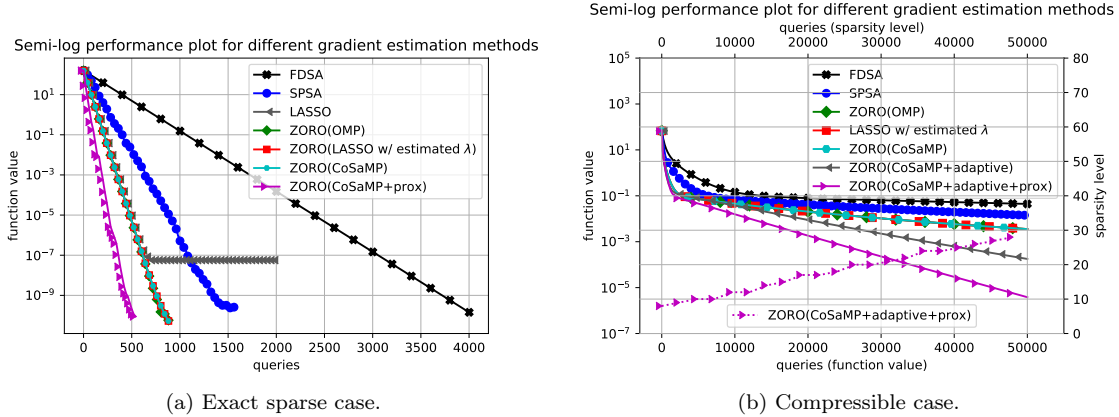


Figure 2: Function values *v.s.* queries for gradient estimation methods in synthetic examples.

Corollary 3.3. Let $F(x) = f(x) + r(x)$ where $f(x)$ satisfies Assumption 3 and $r(x)$ is proximal. Choose $\alpha < 2/L$ if $r(x)$ is convex and $\alpha < 1/L$ if $r(x)$ is non-convex. Let $\{x_1, \dots, x_K\}$ be the iterates found by ZORO after making T oracle queries, where $K = T/m$. Then:

$$\min_{k=1, \dots, K} \|\tilde{\Delta}_k\|_2 \leq \frac{\sqrt{\tilde{c}_5 e_0}}{\sqrt{k+1}} + 2^{3/4} \tilde{c}_6^{1/2} (\tau \sigma H)^{1/4}$$

with probability at least $1 - (s/d)^{b_2 s}$.

4 Numerical experiments

We compared ZORO to gradient-based methods SPSA and FDSA. We did not test any global algorithms (*e.g.*, REMBO [25]) due to their strong correlations with problem structures. Furthermore, we only use Algorithm 3 for CoSaMP gradient estimations in this section, so ZORO does not gain extra advantage with opportunistic gradient estimation.

4.1 Synthetic examples

Consider $f(x) = x^\top A x / 2$, where $A \in \mathbb{R}^{200 \times 200}$ is a diagonal matrix. We tested: (a) exact sparse case with 20 randomly generated diagonal positive numbers; (b) compressible case where diagonal elements are non-zeros that diminish exponentially $A_{i,i} = e^{-\omega i}$ with $\omega = 0.5$.

In case (a), we used ZORO with a proximal operator to enforce non-negative values. The results are shown in Figure 2a. ZORO(CoSaMP+prox) took 1/3 queries of what SPSA needed and 1/8 of FDSA. LASSO with fixed parameter, λ , stopped around $1e-7$ since the ratio between the ℓ_2 -norm squared term and the ℓ_1 term became too small to recover any non-zero gradient. To address this issue, we propose the new parameter: $\lambda_{k+1} = c \|\mathbf{y}_k - Z_k \hat{\mathbf{g}}_k\|_2^2 / \|\hat{\mathbf{g}}_k\|_1$, where c is a fixed parameter. Under this rule, ZORO(LASSO) converged at the same speed as ZORO with other sparse coding methods.

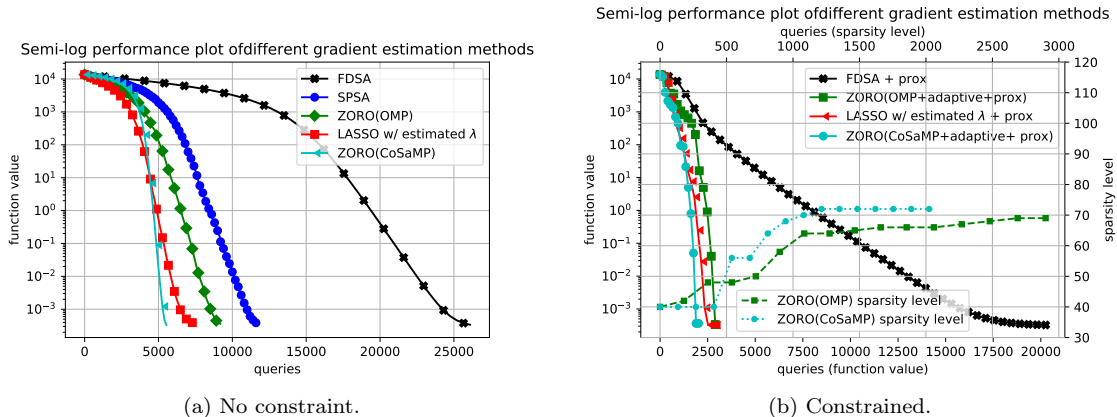


Figure 3: Function values *v.s.* queries for gradient estimation methods in asset risk management.

For case (b), we used the adaptive strategy described in Algorithm 4 to handle growing sparsity level (higher is less compressible). To demonstrate the effect of this adaptive strategy, we use the right y-axis to plot the sparsity levels used at different iterations in Figure 2b.

4.2 Asset risk management

Consider a portfolio consisting of n different assets, where x_i and m_i denote the fraction of the portfolio invested in, and the expected return of, asset i respectively. \mathcal{C} denotes the covariance matrix of asset returns. The portfolio risk, which we aim to minimize, is $\frac{x^\top \mathcal{C} x}{2(\sum_{i=1}^n x_i)^2}$. We used the correlation, mean, and standard deviation of 225 assets from the dataset of [26]. Our goal is to minimize the risk function subject to the expected return constraint $\frac{\sum_{i=1}^n m_i x_i}{\sum_{i=1}^n x_i} > r$. We penalize the risk to formulate the problem as:

$$\underset{x \in \mathbb{R}^n}{\text{minimize}} \frac{x^\top \mathcal{C} x}{2(\sum_{i=1}^n x_i)^2} + \lambda \left(\min \left\{ \frac{\sum_{i=1}^n m_i x_i}{\sum_{i=1}^n x_i} - r, 0 \right\} \right)^2.$$

Instead of solving this quadratic program, consider a problem proposer who wishes to keep the formulation and data private and only offers a noisy zeroth order oracle.

See Figure 3a. When x_i was free (allowing to short), ZORO(CoSaMP) was twice as fast as SPSA and five times as fast as FDSA. All solutions matched the optimal value of quadratic programming. When imposing $x_i \geq 0$ for all i , we implemented the adaptive strategy for both CoSaMP and OMP. We couldn't make SPSA converge. In Figure 3b, we can see that ZORO and LASSO with our adaptive λ were eight times as fast as FDSA. Sparsity level shows that it was enough for ZORO to converge with estimated gradients with only 40–70 nonzeros though each full gradient has 225 nonzeros.

4.3 Sparse adversarial attack on ImageNet

We tested generating black-box adversarial examples using ZORO. We used Inception-V3 model [27] on ImageNet [28] and focused on per-image adversarial attacks. The authors in [29] considered



Figure 4: Examples of adversarial images, true labels, and mis-classified labels.

a similar problem by optimizing the attack loss and the ℓ_2 -norm of image distortion. In contrast, we aimed to find distortions δ for single images x such that the attack loss $f(x + \delta)$ and the ℓ_0 -norm of distortion are minimized: $\text{minimize}_{\delta} f(x + \delta) + \lambda \|\delta\|_0$. All the methods in [29] led to extremely large ℓ_0 distortions, except ZO-SCD, which however had the worse ℓ_2 distortion. Hence, successful attacks required distorting nearly all pixels. We compared ZORO with ZO-AdaMM, ZO-SGD, and ZO-SCD in [29]. ZO-SCD is essentially a variation of FDSA, and ZO-SGD is a mini-batched version of SPSA. We used the same setup in [29]: 10 queries at each iteration and check if the attack succeeds before 1000 iterations. For ZORO, we generated 50 queries at each iteration for sparse recovery and determine if attack succeeds before 200 iterations. In each ZORO iteration, we randomly selected a subspace of 2000 dimensions (pixels) and generated random perturbations only in this subspace. Although sparse adversarial attacks exist (*e.g.*, SparseFool [30]), we appear to be the first to connect adversarial attacks to sparse zeroth-order optimization.

Table 1 presents the experimental results. ZORO had the highest attack success rate while having smaller average ℓ_0 distortion than ZO-SCD. Surprisingly, the average ℓ_2 distortion of ZORO was also the best. The average query of ZORO is the worst as it uses more queries at each iteration. Some pictures of successful sparse attacks by ZORO are presented in Figure 4.

Out of curiosity, we tested applying a median filter, a common method to remove speckle noise, and checked how many adversarial attacks can be mitigated. We used Inception-V3 on the attacked-then-filtered images to check whether true labels are obtained, *i.e.*, mitigated the attacks. We also applied the same filter to the original (un-attacked) images to check if they reduced label accuracies. The results are given in Table 2. While mitigating many attacks, the median filter also distorted the original images, causing lower classification accuracies.

More information about our experiment setting is provided in Appendix E, including the enlarged version of Figure 4.

Acknowledgments

The work of the first two authors was partially supported by NSF Grant DMS-1720237 and ONR Grant N000141712162. The authors would like to thank Drs. Rong Jin and Jian Tan for helpful discussions.

Table 1: Attack success rate (ASR), average final ℓ_0 distortion (as a percentage of the total number of pixels), average final ℓ_2 distortion, and average iterations of first successful attack for different zeroth-order attack methods.

METHODS	ASR	ℓ_0 DIST	ℓ_2 DIST	ITER
ZO-SCD	78 %	0.89%	57.5	240
ZO-SGD	78%	100%	37.9	159
ZO-AdaMM	81%	100%	28.2	172
ZORO	90%	0.73%	21.1	59

Table 2: Recovery success rate (RSR), original image distortion rate, and total prediction accuracy reduction for different median filter sizes.

MEDIAN FILTER	RSR	DIST RATE	TOT REDUCTION
size = 2	86 %	8%	21%
size = 3	92 %	7%	14%
size = 4	76 %	14%	34%
size = 5	69 %	29%	53%

Broader Impact

Our presented algorithm is likely to allow for faster zeroth-order optimization, which can lead to positive benefits in applications such as those mentioned in the introduction. We highlight that the sparse adversarial attacks on ImageNet discussed in Section 4 could be exploited by malicious actors. However, it is our hope that knowledge of the existence of this attack could aid researchers in constructing more robust classification algorithms.

References

- [1] Ben Taskar, Vassil Chatalbashev, Daphne Koller, and Carlos Guestrin. Learning structured prediction models: A large margin approach. In *Proceedings of the 22nd international conference on Machine learning*, pages 896–903, 2005.
- [2] Krzysztof Choromanski, Mark Rowland, Vikas Sindhwani, Richard E Turner, and Adrian Weller. Structured evolution with compact architectures for scalable policy optimization. *arXiv preprint arXiv:1804.02395*, 2018.
- [3] Abraham D Flaxman, Adam Tauman Kalai, and H Brendan McMahan. Online convex optimization in the bandit setting: gradient descent without a gradient. *arXiv preprint cs/0408007*, 2004.

- [4] Ohad Shamir. On the complexity of bandit and derivative-free stochastic convex optimization. In *Conference on Learning Theory*, pages 3–24, 2013.
- [5] Nathan Nakamura, Jason Seepaul, Joseph B Kadane, and B Reeja-Jayan. Design for low-temperature microwave-assisted crystallization of ceramic thin films. *Applied Stochastic Models in Business and Industry*, 33(3):314–321, 2017.
- [6] Alexey Kurakin, Ian Goodfellow, and Samy Bengio. Adversarial machine learning at scale. *arXiv preprint arXiv:1611.01236*, 2016.
- [7] Nicolas Papernot, Patrick McDaniel, Ian Goodfellow, Somesh Jha, Z Berkay Celik, and Ananthram Swami. Practical black-box attacks against machine learning. In *Proceedings of the 2017 ACM on Asia conference on computer and communications security*, pages 506–519, 2017.
- [8] Jasper Snoek, Hugo Larochelle, and Ryan P Adams. Practical bayesian optimization of machine learning algorithms. In *Advances in neural information processing systems*, pages 2951–2959, 2012.
- [9] Jack Kiefer, Jacob Wolfowitz, et al. Stochastic estimation of the maximum of a regression function. *The Annals of Mathematical Statistics*, 23(3):462–466, 1952.
- [10] James C Spall. An overview of the simultaneous perturbation method for efficient optimization. *Johns Hopkins apl technical digest*, 19(4):482–492, 1998.
- [11] Yurii Nesterov and Vladimir Spokoiny. Random gradient-free minimization of convex functions. *Technical report, Universite catholique de Louvain, Center for Operations Research and Econometrics (CORE)*, 2011.
- [12] Alekh Agarwal, Ofer Dekel, and Lin Xiao. Optimal algorithms for online convex optimization with multi-point bandit feedback. In *COLT*, pages 28–40. Citeseer, 2010.
- [13] John C Duchi, Michael I Jordan, Martin J Wainwright, and Andre Wibisono. Optimal rates for zero-order convex optimization: The power of two function evaluations. *IEEE Transactions on Information Theory*, 61(5):2788–2806, 2015.
- [14] Yining Wang, Simon Du, Sivaraman Balakrishnan, and Aarti Singh. Stochastic zeroth-order optimization in high dimensions. In *International Conference on Artificial Intelligence and Statistics*, pages 1356–1365, 2018.
- [15] Saeed Ghadimi and Guanghui Lan. Stochastic first-and zeroth-order methods for nonconvex stochastic programming. *SIAM Journal on Optimization*, 23(4):2341–2368, 2013.
- [16] Xiangru Lian, Huan Zhang, Cho-Jui Hsieh, Yijun Huang, and Ji Liu. A comprehensive linear speedup analysis for asynchronous stochastic parallel optimization from zeroth-order to first-order. In *Advances in Neural Information Processing Systems*, pages 3054–3062, 2016.
- [17] Bin Gu, Zhouyuan Huo, Cheng Deng, and Heng Huang. Faster derivative-free stochastic algorithm for shared memory machines. In *International Conference on Machine Learning*, pages 1812–1821, 2018.

- [18] Krishnakumar Balasubramanian and Saeed Ghadimi. Zeroth-order (non)-convex stochastic optimization via conditional gradient and gradient updates. In *Advances in Neural Information Processing Systems*, pages 3455–3464, 2018.
- [19] Yurii Nesterov and Vladimir Spokoiny. Random gradient-free minimization of convex functions. *Foundations of Computational Mathematics*, 17(2):527–566, 2017.
- [20] Kevin G Jamieson, Robert Nowak, and Ben Recht. Query complexity of derivative-free optimization. In *Advances in Neural Information Processing Systems*, pages 2672–2680, 2012.
- [21] Jeffrey Larson, Matt Menickelly, and Stefan M Wild. Derivative-free optimization methods. *Acta Numerica*, 28:287–404, 2019.
- [22] Deanna Needell and Joel A Tropp. Cosamp: Iterative signal recovery from incomplete and inaccurate samples. *Applied and computational harmonic analysis*, 26(3):301–321, 2009.
- [23] Jianqing Fan and Runze Li. Variable selection via nonconcave penalized likelihood and its oracle properties. *Journal of the American statistical Association*, 96(456):1348–1360, 2001.
- [24] Simon Foucart. Sparse recovery algorithms: sufficient conditions in terms of restricted isometry constants. In *Approximation Theory XIII: San Antonio 2010*, pages 65–77. Springer, 2012.
- [25] Ziyu Wang, Masrour Zoghi, Frank Hutter, David Matheson, and Nando De Freitas. Bayesian optimization in high dimensions via random embeddings. In *Twenty-Third International Joint Conference on Artificial Intelligence*, 2013.
- [26] T-J Chang, Nigel Meade, John E Beasley, and Yazid M Sharaiha. Heuristics for cardinality constrained portfolio optimisation. *Computers & Operations Research*, 27(13):1271–1302, 2000.
- [27] Christian Szegedy, Vincent Vanhoucke, Sergey Ioffe, Jon Shlens, and Zbigniew Wojna. Rethinking the inception architecture for computer vision. In *Proceedings of the IEEE conference on computer vision and pattern recognition*, pages 2818–2826, 2016.
- [28] Jia Deng, Wei Dong, Richard Socher, Li-Jia Li, Kai Li, and Li Fei-Fei. Imagenet: A large-scale hierarchical image database. In *2009 IEEE conference on computer vision and pattern recognition*, pages 248–255. Ieee, 2009.
- [29] Xiangyi Chen, Sijia Liu, Kaidi Xu, Xingguo Li, Xue Lin, Mingyi Hong, and David Cox. Zoadamm: Zeroth-order adaptive momentum method for black-box optimization. In *Advances in Neural Information Processing Systems*, pages 7202–7213, 2019.
- [30] Apostolos Modas, Seyed-Mohsen Moosavi-Dezfooli, and Pascal Frossard. Sparsefool: a few pixels make a big difference. In *Proceedings of the IEEE Conference on Computer Vision and Pattern Recognition*, pages 9087–9096, 2019.
- [31] Frank Schöpfer. Linear convergence of descent methods for the unconstrained minimization of restricted strongly convex functions. *SIAM Journal on Optimization*, 26(3):1883–1911, 2016.
- [32] Hui Zhang. The restricted strong convexity revisited: analysis of equivalence to error bound and quadratic growth. *Optimization Letters*, 11(4):817–833, 2017.

- [33] Richard Baraniuk, Mark Davenport, Ronald DeVore, and Michael Wakin. A simple proof of the restricted isometry property for random matrices. *Constructive Approximation*, 28(3):253–263, 2008.
- [34] Michael P Friedlander and Mark Schmidt. Hybrid deterministic-stochastic methods for data fitting. *SIAM Journal on Scientific Computing*, 34(3):A1380–A1405, 2012.

ZORO: Supplemental Materials

In this supplementary material we provide the definitions and the proofs for the main theorems presented in the main article and present the results of some additional numerical experiments. Specifically, in Section A, we provide standard definition for the terminologies we used in this paper. In Section B we present the proofs for Section 2 in the main article, which center around the accuracy of the gradient estimator used in ZORO. Section C contains several technical results on sequences and inexact gradient descent, and culminates in the proofs of Theorems C.1 and C.2. In Section D we present the proofs of our main results, namely those contained in section 3, while in Section E we present some additional numerical results that may be of interest.

Before proceeding, for the reader's convenience, we provide a table of notation here (see Table 3).

A Definitions

Definition 1 (Convexity). A function h is *convex* if for all $x, y \in \mathbb{R}^d$ and $t \in [0, 1]$, it holds:

$$h(tx + (1 - t)y) \leq th(x) + (1 - t)h(y). \quad (7)$$

Additionally, if h is differentiable, then (7) is equivalent to

$$h(y) \geq h(x) + \nabla h(x)^\top (y - x). \quad (8)$$

Definition 2 (Restricted strong convexity). A function h is *restricted ν -strongly convex* if

$$h(x) - \min h \geq \nu \|x - P_*(x)\|_2^2 \quad (9)$$

for all $x \in \mathbb{R}^d$, where $P_*(\cdot)$ is a projection operator onto the solution set defined by $P_*(x) := \operatorname{argmin}_{y \in \text{solution set of } h} \|y - x\|_2$.

One can see Definition 2 is indeed weaker than the commonly used strong convexity. We refer the interested readers to [31, 32] for more results.

Definition 3 (Coercivity). 1. A function $h : \mathbb{R}^d \rightarrow \mathbb{R}$ is *coercive* if $\lim_{\|x\|_2 \rightarrow \infty} h(x) = +\infty$.
 2. More generally, a function $h : \mathbb{R}^d \rightarrow \mathbb{R}$ is *coercive with respect to* $g : \mathbb{R}^d \rightarrow \mathbb{R}$ if for any $\{x_k\}_{k=1}^\infty$ satisfying $\lim_{k \rightarrow \infty} g(x_k) = +\infty$, we also have $\lim_{k \rightarrow \infty} h(x_k) = +\infty$.
 3. Finally, a set-valued operator A on \mathbb{R}^d is *coercive with respect to* $g : \mathbb{R}^d \rightarrow \mathbb{R}$ if for any $\{x_k\}_{k=1}^\infty$ satisfying $\lim_{k \rightarrow \infty} g(x_k) = +\infty$, we also have $\lim_{k \rightarrow \infty} \inf_{y \in A(x_k)} \|y\|_2 = +\infty$.

If r is a closed proper convex function, then

$$\mathbf{prox}_{\alpha r}(y) := \operatorname{argmin}_{x \in \mathbb{R}^d} r(x) + \frac{1}{2\alpha} \|x - y\|_2^2. \quad (10)$$

is well-defined. More generally:

Definition 4 (Proximability). r is *proximable* if $\mathbf{prox}_{\alpha r}(y)$ in (10) is a single-valued operator.

Table 3: Table of Notation.

NOTATION	DEFINITION
d	dimension of x
$f(x)$	underlying loss function
s	sparsity of ∇f (when it is sparse)
$r(x)$	regularization function
$F(x)$	$f(x) + r(x)$, if r is non-zero
$\min F$	$\min\{F(x) : x \in \mathbb{R}^d\}$, minimum value of F
e_k	$F(x_k) - \min F$, objective error
x_k	k -th iterate of ZORO
z_i	Rademacher random variable
n	number of iterations of CoSaMP in ZORO
\mathbf{g}_k	$\nabla f(x_k)$, true gradient at x_k
$\hat{\mathbf{g}}_k$	estimated gradient at x_k
\mathbf{e}_k	$\hat{\mathbf{g}}_k - \mathbf{g}_k$, gradient estimation error
$\tilde{\nabla} r$	∂r picked out by the proximal operator
$\hat{\Delta}_k$	$-(\tilde{\nabla} r(x_{k+1}) + \hat{\mathbf{g}}_k)$
Δ_k	$-(\tilde{\nabla} r(x_{k+1}) + \mathbf{g}_k)$
$\hat{\Delta}_k$	$-(\tilde{\nabla} r(x_{k+1}) + \mathbf{g}_{k+1})$
H	uniform bound of $\ \nabla^2 f\ _1$ (Asm. 2)
L	Lipschitz constant of ∇f (Asm. 3)
ν	restricted strong convexity of f (Def. 2)
$E_f(x)$	oracle query of $f(x)$, see (2)
ξ	oracle noise
σ	bound of ξ (Asm. 4)
m	number of samples
δ	sampling radius, see (5)
$\ \cdot\ _0$	ℓ_0 -norm
$\ \cdot\ _1$	ℓ_1 -norm
$\ \cdot\ _2$	ℓ_2 -norm
$\ \cdot\ _\infty$	ℓ_∞ -norm
$[\cdot]_{(s)}$	best s -sparse approximate
$\mathbf{P}_*(\cdot)$	projection onto the solution set
$\mathbb{P}[\cdot]$	probability
$\mathbb{E}[\cdot]$	expectation

B Lemmas and Proofs for Gradient Estimation

Here we provide proofs and supporting results for Theorems 2.1 and 2.2. We start with a lemma characterizing the error in our measurements.

Lemma B.1. *If Assumptions 2 and 4 are satisfied, then*

$$y_i = \frac{1}{\sqrt{m}} z_i^\top \mathbf{g} + \frac{\mu_i}{\delta} + \delta \nu_i$$

with $\mathbf{g} = \nabla f(x)$, $|\mu_i| \leq 2\sigma/\sqrt{m}$, and $|\nu_i| \leq H/(2\sqrt{m})$.

Proof of Lemma B.1. The proof is similar to the argument of Section 3 in [14], but we include it for completeness. From Taylor's theorem:

$$f(x + \delta z_i) = f(x) + \delta z_i^\top \mathbf{g} + \frac{\delta^2}{2} z_i^\top \nabla^2 f(x + tz_i) z_i$$

for some $t \in (0, 1)$. Assuming $E_f(x + \delta z_i) = f(x + \delta z_i) + \xi_+$ and $E_f(x) = f(x) + \xi_-$, equation (5) becomes:

$$\begin{aligned} y_i &= \frac{1}{\sqrt{m}} z_i^\top \mathbf{g} + \frac{\xi_+ - \xi_-}{\sqrt{m}} \\ &\quad + \frac{\delta}{2\sqrt{m}} z_i^\top \nabla^2 f(x + tz_i) z_i. \end{aligned}$$

Let $\mu_i := \frac{\xi_+ - \xi_-}{\sqrt{m}}$, then $|\mu_i| \leq 2\sigma/\sqrt{m}$. Let $\nu_i = z_i^\top \nabla^2 f(x + tz_i) z_i / (2\sqrt{m})$. Now:

$$\begin{aligned} 2\sqrt{m}|\nu_i| &= |z_i^\top \nabla^2 f(x + t_0 \delta z_i) z_i| \\ &= \left| \sum_{j,k} \nabla_{j,k}^2 f(x + t_0 \delta z_i) (z_i)_j (z_i)_k \right| \\ &\leq \|\nabla^2 f(x + t_0 \delta z_i)\|_1 \|z_i\|_\infty^2 \leq H \end{aligned}$$

by Assumption 2 and the fact that $\|z_i\|_\infty = 1$. □

For future use, let $\boldsymbol{\mu} = [\mu_1, \dots, \mu_m]^\top$ and $\boldsymbol{\nu} = [\nu_1, \dots, \nu_m]^\top$. Then:

$$\mathbf{y} = Z\mathbf{g} + \frac{1}{\delta}\boldsymbol{\mu} + \delta\boldsymbol{\nu}. \tag{11}$$

Let us now recall a few theorems from the compressive sensing literature that will be of use.

Theorem B.2 (Theorem 5.2 of [33]). *If $m = b_1 s \log(d/s)$ then Z satisfies the Restricted Isometry Property (RIP) with constant $\delta_{4s}(Z) \leq 0.3843$ with probability $1 - (s/d)^{b_2 s}$. Here b_1 and b_2 are constants independent of s, d and m .*

We remind the reader that Z has the $(4s)$ -RIP if, for all $\mathbf{v} \in \mathbb{R}^d$ with $\|\mathbf{v}\|_0 \leq 4s$:

$$(1 - \delta_{4s}(Z))\|\mathbf{v}\|_2^2 \leq \|Z\mathbf{v}\|_2^2 \leq (1 + \delta_{4s}(Z))\|\mathbf{v}\|_2^2.$$

The choice of the value 0.3843 is to match with the assumptions of [24], the main result of which we state next. Recall that $[\mathbf{g}]_{(s)}$ denotes the best s -sparse approximation to \mathbf{g} .

Theorem B.3 (Theorem 5 of [24]). *Let $\{\mathbf{g}^n\}$ be the sequence generated by applying CoSaMP [22] to problem (6), with $m \geq b_1 s \log(d/s)$ and initialization $\mathbf{g}^0 = \mathbf{0}$. Then, with probability $1 - (s/d)^{b_2 s}$: for all \mathbf{g} ,*

$$\left\| \mathbf{g}^n - [\mathbf{g}]_{(s)} \right\|_2 \leq \tau \left\| Z(\mathbf{g} - [\mathbf{g}]_{(s)}) + \frac{1}{\delta} \boldsymbol{\mu} + \delta \boldsymbol{\nu} \right\|_2 + \rho^n \left\| [\mathbf{g}]_{(s)} \right\|_2, \quad (12)$$

where $\rho < 1$ and $\tau \approx 10$ depend only on δ_{4s} .

The exact values of ρ and τ are provided in [24]. Note that the constants b_1, b_2 are the same as in Theorem B.2. Certainly, other initializations are possible. For example, when using the ZORO method we have found that taking \mathbf{g}^0 to be the gradient estimator found at the previous step, *i.e.*, $\mathbf{g}^0 = \hat{\mathbf{g}}_{k-1}$, offers a modest speed-up.

Theorem B.4 (Proposition 3.5 in [22]). *Suppose that Z satisfies the (4s)-RIP. Then for any $\mathbf{v} \in \mathbb{R}^d$:*

$$\|Z\mathbf{v}\|_2 \leq \sqrt{1 + \delta_{4s}(Z)} \left(\|\mathbf{v}\|_2 + \frac{1}{\sqrt{s}} \|\mathbf{v}\|_1 \right).$$

Theorem B.5 (Concentration of measure). *Suppose that $Z = \frac{1}{\sqrt{m}} A \in \mathbb{R}^{m \times d}$ where:*

$$A_{ij} = \begin{cases} +1 & \text{with probability } 1/2, \\ -1 & \text{with probability } 1/2. \end{cases}$$

Then for any $\varepsilon > 0$ and any $\mathbf{v} \in \mathbb{R}^d$:

$$\mathbb{P} \left[\left| \|Z\mathbf{v}\|_2^2 - \|\mathbf{v}\|_2^2 \right| \geq \varepsilon \|\mathbf{v}\|_2^2 \right] \leq 2e^{-mb_3(\varepsilon)}$$

where $b_3(\varepsilon) := \varepsilon^2/4 - \varepsilon^3/6$.

Proof. See, for example, [33] and references contained therein. □

Note that it follows from (12) that:

$$\|\mathbf{g}^n - \mathbf{g}\|_2 \leq \|\mathbf{g} - [\mathbf{g}]_{(s)}\|_2 + \tau \|Z(\mathbf{g} - [\mathbf{g}]_{(s)})\|_2 + \frac{\tau}{\delta} \|\boldsymbol{\mu}\|_2 + \tau \delta \|\boldsymbol{\nu}\|_2 + \rho^n \|\mathbf{g}\|_2. \quad (13)$$

Lemma B.6. *Suppose ∇f is compressible. Then $\|\mathbf{g} - [\mathbf{g}]_{(s)}\|_2 + \tau \|Z(\mathbf{g} - [\mathbf{g}]_{(s)})\|_2 \leq \psi \|\mathbf{g}\|_2$ where:*

$$\psi = \left(\left(1 + \tau \sqrt{1 + \delta_{4s}(Z)} \right) \left(\frac{2}{p} - 1 \right)^{-1/2} + \tau \sqrt{1 + \delta_{4s}(Z)} \left(\frac{1}{p} - 1 \right)^{-1} \right) s^{1/2-1/p}.$$

Proof. Combining the bounds (3),(4) and Theorem B.4 we obtain:

$$\begin{aligned} \|Z(\mathbf{g} - [\mathbf{g}]_{(s)})\|_2 &\leq \sqrt{1 + \delta_{4s}(Z)} \left(\|\mathbf{g} - [\mathbf{g}]_{(s)}\|_2 + \frac{1}{\sqrt{s}} \|\mathbf{g} - [\mathbf{g}]_{(s)}\|_1 \right) \\ &\leq \sqrt{1 + \delta_{4s}(Z)} \left(\left(\frac{2}{p} - 1 \right)^{-1/2} \|\mathbf{g}\|_2 s^{1/2-1/p} + \frac{1}{\sqrt{s}} \left(\frac{1}{p} - 1 \right)^{-1} \|\mathbf{g}\|_2 s^{1-1/p} \right) \\ &= \sqrt{1 + \delta_{4s}(Z)} \left(\left(\frac{2}{p} - 1 \right)^{-1/2} + \left(\frac{1}{p} - 1 \right)^{-1} \right) s^{1/2-1/p} \|\mathbf{g}\|_2. \end{aligned}$$

Use (4) again to bound $\|\mathbf{g} - [\mathbf{g}]_{(s)}\|_2$ and add to obtain the lemma. □

Returning to the problem at hand, we are able to bound the magnitude of the error terms in our measurements:

Lemma B.7. $\|\boldsymbol{\mu}\|_2 \leq 2\sigma$ and $\|\boldsymbol{\nu}\|_2 \leq H/2$.

Proof. From Lemma B.1, we have

$$\|\boldsymbol{\mu}\|_2^2 = \sum_{i=1}^m \mu_i^2 \leq \sum_{i=1}^m \frac{4\sigma^2}{m} = 4\sigma^2.$$

Similarly, we also get

$$\|\boldsymbol{\nu}\|_2^2 = \sum_{i=1}^m \nu_i^2 \leq \sum_{i=1}^m \frac{H^2}{4m} = \frac{H^2}{4}.$$

□

Combining Lemmas B.6 and B.7 with (13), and using $\|[\mathbf{g}]_{(s)}\|_2 \leq \|\mathbf{g}\|_2$, yields the following master theorem that generically bounds the gradient estimation error of Algorithm 3.

Theorem B.8. *Generate $\{z_i\}_{i=1}^m$ as described in Algorithm 1. Suppose further that Assumptions 1, 2 and 4 are satisfied. Then with probability at least $1 - (s/d)^{b_2 s}$:*

$$\|\hat{\mathbf{g}} - \mathbf{g}\|_2 \leq (\psi + \rho^n) \|\mathbf{g}\|_2 + \frac{2\tau\sigma}{\delta} + \frac{\tau\delta H}{2},$$

for all $x \in \mathbb{R}^d$, where $\hat{\mathbf{g}}$ denotes the output after n iterations of CoSaMP applied to problem (6) and b_2 is defined as in Lemma B.2. Here $\rho < 1$ and $\tau \approx 15$ are fixed numerical constants, and:

$$\psi = \begin{cases} 0 & \text{if } \nabla f(x) \text{ is } s\text{-sparse,} \\ Cs^{1/2-1/p} & \text{if } \nabla f(x) \text{ is compressible.} \end{cases}$$

Note that C depends on p and $\{z_i\}_{i=1}^m$, but not on s .

Proofs of Theorems 2.1 and 2.2 are then derived by specializing Theorem B.8.

Proof of Theorem 2.1. Applying Theorem B.8 with $\sigma = 0$ yields

$$\begin{aligned} \|\mathbf{g}_k - \hat{\mathbf{g}}_k\|_2 &\leq \frac{\tau\delta_k H}{2} + (\psi + \rho^n) \|\mathbf{g}_k\|_2 \\ &= \left(\frac{\tau\delta_k H}{2(\varepsilon_{\text{rel}} - \psi - \rho^n) \|\mathbf{g}_k\|_2} \right) (\varepsilon_{\text{rel}} - \psi - \rho^n) \|\mathbf{g}_k\|_2 + (\psi + \rho^n) \|\mathbf{g}_k\|_2, \end{aligned}$$

for all k with probability $1 - (s/d)^{b_2 s}$. Now, to guarantee that $\|\mathbf{g}_k - \hat{\mathbf{g}}_k\|_2 \leq \varepsilon_{\text{rel}} \|\mathbf{g}_k\|_2$ we need to choose

$$\delta_k \leq \frac{2(\varepsilon_{\text{rel}} - \psi - \rho^n) \|\mathbf{g}_k\|_2}{\tau H}. \quad (14)$$

Of course, we do not have access to $\|\mathbf{g}_k\|_2$ when choosing δ_k ; hence, we use $\|\hat{\mathbf{g}}_{k-1}\|_2$ as a proxy. We use the inductive assumption that $\|\mathbf{g}_{k-1} - \hat{\mathbf{g}}_{k-1}\|_2 \leq \varepsilon_{\text{rel}} \|\mathbf{g}_{k-1}\|_2$, in which case we have that:

$$\begin{aligned} \|\hat{\mathbf{g}}_{k-1}\|_2 &= \|\hat{\mathbf{g}}_{k-1} - \mathbf{g}_{k-1} + \mathbf{g}_{k-1} - \mathbf{g}_k + \mathbf{g}_k\|_2 \\ &\leq \|\hat{\mathbf{g}}_{k-1} - \mathbf{g}_{k-1}\|_2 + \|\mathbf{g}_{k-1} - \mathbf{g}_k\|_2 + \|\mathbf{g}_k\|_2 \\ &\leq \varepsilon_{\text{rel}} \|\mathbf{g}_{k-1}\|_2 + L\|x_k - x_{k-1}\|_2 + \|\mathbf{g}_k\|_2 \end{aligned} \quad (15)$$

Because $x_k = x_{k-1} - \alpha \hat{\mathbf{g}}_{k-1}$ we have that $L\|x_k - x_{k-1}\|_2 \leq \alpha L \|\hat{\mathbf{g}}_{k-1}\|_2$. Moreover, one can easily show that:

$$\|\mathbf{g}_{k-1}\|_2 \leq \frac{1}{1 - \varepsilon_{\text{rel}}} \|\hat{\mathbf{g}}_{k-1}\|_2$$

Thus equation (15) becomes

$$\begin{aligned} \|\hat{\mathbf{g}}_{k-1}\|_2 &\leq \frac{\varepsilon_{\text{rel}}}{1 - \varepsilon_{\text{rel}}} \|\hat{\mathbf{g}}_{k-1}\|_2 + \alpha L \|\hat{\mathbf{g}}_{k-1}\|_2 + \|\mathbf{g}_k\|_2 \\ \Rightarrow \left(\frac{1 - \alpha L - \varepsilon_{\text{rel}}(2 - \alpha L)}{1 - \varepsilon_{\text{rel}}} \right) \|\hat{\mathbf{g}}_{k-1}\|_2 &\leq \|\mathbf{g}_k\|_2 \end{aligned}$$

and so to guarantee (14), it suffices to choose

$$\begin{aligned} \delta_k &\leq \frac{2(\varepsilon_{\text{rel}} - \psi - \rho^n)(1 - L\alpha - \varepsilon_{\text{rel}}(2 - \alpha L))}{\tau H(1 - \varepsilon_{\text{rel}})} \|\hat{\mathbf{g}}_{k-1}\|_2 \\ &=: \beta \|\hat{\mathbf{g}}_{k-1}\|_2. \end{aligned}$$

Note that this condition is only meaningful when $\beta > 0$, thus we require that:

$$\psi + \rho^n < \varepsilon_{\text{rel}} < \frac{1 - \alpha L}{2 - \alpha L} \quad \text{and} \quad \alpha < \frac{1}{L}.$$

□

Theorem 2.1 requires that $\|\mathbf{g}_0 - \hat{\mathbf{g}}_0\|_2 \leq \varepsilon_{\text{rel}} \|\mathbf{g}_0\|_2$. Let us briefly discuss how one can guarantee this. From Theorem B.5 we get that with probability $1 - e^{-m/24}$:

$$\begin{aligned} \|Z(\mathbf{g}_0 - \hat{\mathbf{g}}_0)\|_2^2 &\geq \frac{1}{2} \|\mathbf{g}_0 - \hat{\mathbf{g}}_0\|_2^2 \\ \Rightarrow \|\mathbf{g}_0 - \hat{\mathbf{g}}_0\|_2 &\leq \sqrt{2} \|Z\mathbf{g}_0 - Z\hat{\mathbf{g}}_0\|_2 \\ &\stackrel{(a)}{=} \sqrt{2} \|(\mathbf{y} + \delta\boldsymbol{\nu}) - Z\hat{\mathbf{g}}_0\|_2 \\ &\stackrel{(b)}{\leq} \sqrt{2} \left(\|\mathbf{y} - Z\hat{\mathbf{g}}_0\|_2 + \frac{H\delta}{2} \right) \end{aligned}$$

where (a) follows from (11) with $\sigma = 0$ and (b) follows from Lemma B.7. On the other hand:

$$\begin{aligned} \|\mathbf{y}\|_2 &\stackrel{(a)}{=} \|Z\mathbf{g}_0 + \delta\boldsymbol{\nu}\|_2 \\ &\stackrel{(b)}{\leq} \|Z\mathbf{g}_0\|_2 + \frac{H\delta}{2} \\ &\stackrel{(c)}{\leq} \sqrt{2} \|\mathbf{g}_0\|_2 + \frac{H\delta}{2}, \end{aligned}$$

where again (a) follows from (11) and (b) from Lemma B.7 while (c) holds with probability $1 - e^{-m/12}$ by Theorem B.5. It follows that:

$$\frac{1}{\sqrt{2}} \left(\|\mathbf{y}\|_2 - \frac{H\delta}{2} \right) \leq \|\mathbf{g}_0\|_2$$

and thus if:

$$\begin{aligned} \sqrt{2} \left(\|\mathbf{y} - Z\hat{\mathbf{g}}_0\|_2 + \frac{H\delta}{2} \right) &\leq \frac{\varepsilon_{\text{rel}}}{\sqrt{2}} \left(\|\mathbf{y}\|_2 - \frac{H\delta}{2} \right) \\ \iff \|\mathbf{y} - Z\hat{\mathbf{g}}_0\|_2 &\leq \frac{\varepsilon_{\text{rel}}}{2} \|\mathbf{y}\|_2 - \left(1 + \frac{\varepsilon_{\text{rel}}}{2} \right) \left(\frac{H\delta}{2} \right), \end{aligned}$$

then with probability $1 - e^{-m/12} - e^{-m/24}$ we indeed have that $\|\mathbf{g}_0 - \hat{\mathbf{g}}_0\|_2 \leq \varepsilon_{\text{rel}}\|\mathbf{g}_0\|_2$. This condition is checkable, assuming we have a good estimate of H . Furthermore, it must hold for δ sufficiently small. Thus, we recommend starting with some initial estimate δ_0 and performing a decreasing binary search over $(0, \delta_0)$ until a δ is found such that this condition holds.

Proof of Theorem 2.2. From Theorem B.8 we obtain:

$$\|\mathbf{g}_k - \hat{\mathbf{g}}_k\|_2 \leq \frac{2\tau\sigma}{\delta} + \frac{\tau\delta H}{2} + \rho^n \|\mathbf{g}_k\|_2$$

for all k with probability $1 - (s/d)^{b_2 s}$. . Because \mathbf{g}_k is s -sparse:

$$\begin{aligned} \|\mathbf{g}_k\|_2 &\stackrel{(a)}{\leq} \frac{1}{\sqrt{1 - \delta_s(Z)}} \|Z\mathbf{g}_k\|_2 \\ &\stackrel{(b)}{\leq} \frac{1}{\sqrt{1 - \delta_s(Z)}} (\|\mathbf{y}_k\|_2 + \delta_k \|\boldsymbol{\nu}\|_2) \\ &\stackrel{(c)}{\leq} \frac{1}{\sqrt{1 - \delta_s(Z)}} \left(\|\mathbf{y}_k\|_2 + \frac{\delta_k H}{2} \right) \\ &\stackrel{(d)}{\leq} \sqrt{2} \left(\|\mathbf{y}_k\|_2 + \frac{\delta_k H}{2} \right) \end{aligned}$$

where (a) follows from the definition of the RIP (see discussion below Theorem B.2), (b) follows from (11), (c) follows from Lemma B.7 and (d) is because $\delta_s(Z) \leq \delta_{4s}(Z) \leq 0.5$ by Theorem B.2.

Choosing n sufficiently large (specifically $n = \frac{\log(\delta H/2) - \log(\sqrt{2}(\|\mathbf{y}\|_k + \delta_k H/2))}{\log(\rho)}$) we obtain:

$$\|\mathbf{g}_k - \hat{\mathbf{g}}_k\|_2 \leq \frac{2\tau\sigma}{\delta} + \tau\delta H$$

Optimizing the right hand side in terms of δ we obtain that $\|\mathbf{g} - \hat{\mathbf{g}}\|_2 \leq 2\sqrt{2\tau\sigma H}$ and that this is achieved when $\delta = \sqrt{2\sigma/H}$ \square

C Convergence analysis for inexact (projected) gradient descent

Recall the sequence produced by ZORO can be written as:

$$x_{k+1} = \text{prox}_{\alpha r}(x_k - \alpha \hat{\mathbf{g}}_k). \tag{16}$$

Algorithm 4 Opportunistic Gradient Estimation (OppGradEst)

- 1: **Input:** x : current point; \hat{S}_{k-1} : support of $\hat{\mathbf{g}}_{k-1}$; δ : query radius; $\{z_i\}_{i=1}^m$: sample directions; ϕ : error tolerance.
 - 2: $s \leftarrow |\hat{S}_{k-1}|$
 - 3: $\mathbf{y} \leftarrow \text{Sample}(x, \delta, \{z_i\}_{i=1}^s)$ (see Alg. 2)
 - 4: $Z \leftarrow [z_1, \dots, z_s]^\top$
 - 5: $\hat{\mathbf{g}} \leftarrow \text{argmin}_{\mathbf{g}} \|Z\mathbf{g} - \mathbf{y}\|_2$ s.t. $\text{supp}(\mathbf{g}) = \hat{S}_{k-1}$
 - 6: **if** $\|Z\hat{\mathbf{g}} - \mathbf{y}\|_2 / \|\mathbf{y}\|_2 \leq \phi$ **then**
 - 7: **Terminate algorithm and output**
 - 8: **end if**
 - 9: $\mathbf{y} \leftarrow \frac{1}{\sqrt{m}}[\mathbf{y}; \text{Sample}(x, \delta, \{z_i\}_{i=s+1}^m)]$
 - 10: $Z \leftarrow \frac{1}{\sqrt{m}}[z_1, \dots, z_m]^\top$
 - 11: $\hat{\mathbf{g}} \approx \text{argmin}_{\|\mathbf{g}\|_0 \leq s} \|Z\mathbf{g} - \mathbf{y}\|_2$ by CoSaMP
 - 12: **while** $\|Z\hat{\mathbf{g}} - \mathbf{y}\|_2 / \|\mathbf{y}\|_2 > \phi$ **do**
 - 13: $m^{\text{new}} \leftarrow m + \log(d/s)$
 - 14: Generate Rademacher random vectors $z_{m+1}, \dots, z_{m^{\text{new}}}$
 - 15: $\mathbf{y} \leftarrow \frac{1}{\sqrt{m^{\text{new}}}}[\sqrt{m}\mathbf{y}; \text{Sample}(x, \delta, \{z_i\}_{i=m+1}^{m^{\text{new}}})]$
 - 16: $Z \leftarrow \frac{1}{\sqrt{m^{\text{new}}}}[\sqrt{m}Z^\top, z_{m+1}, \dots, z_{m^{\text{new}}}]^\top$
 - 17: $m \leftarrow m^{\text{new}}$ and $s \leftarrow s + 1$
 - 18: $\hat{\mathbf{g}} \approx \text{argmin}_{\|\mathbf{g}\|_0 \leq s} \|Z\mathbf{g} - \mathbf{y}\|_2$ by CoSaMP
 - 19: **end while**
 - 20: **Output:** $\hat{\mathbf{g}}, \{z_i\}_{i=1}^m$
-

Note that if $r(x) = 0$ (i.e., there is no regularization), then (16) reduces to (inexact) gradient descent: $x_{k+1} = x_k - \alpha \hat{\mathbf{g}}_k$. In the case where $r(x) \neq 0$ we may write:

$$x_{k+1} = x_k - \alpha \underbrace{(\tilde{\nabla} r(x_{k+1}) + \hat{\mathbf{g}}_k)}_{-\Delta_k}, \quad (17)$$

where $\tilde{\nabla} r(x_{k+1}) = \frac{1}{\alpha}((x_k - \alpha \hat{\mathbf{g}}_k) - \mathbf{prox}_{\alpha r}(x_k - \alpha \hat{\mathbf{g}}_k)) \in \partial r(x_{k+1})$ is the subgradient picked out by the proximal operator. Moreover, we define

$$\begin{aligned} \text{Actual direction:} & \quad \hat{\Delta}_k := -(\tilde{\nabla} r(x_{k+1}) + \hat{\mathbf{g}}_k), \\ \text{Ideal direction:} & \quad \Delta_k := -(\tilde{\nabla} r(x_{k+1}) + \mathbf{g}_k), \\ \text{Stationarity:} & \quad \tilde{\Delta}_k := -(\tilde{\nabla} r(x_{k+1}) + \mathbf{g}_{k+1}). \end{aligned}$$

Note $\hat{\Delta}_k = \frac{1}{\alpha}(x_{k+1} - x_k)$. The three quantities have the following relations:

$$\left| \|\hat{\Delta}_k\|_2 - \|\Delta_k\|_2 \right| \leq \|\hat{\mathbf{g}}_k - \mathbf{g}_k\|_2, \quad (18)$$

$$\left| \|\tilde{\Delta}_k\|_2 - \|\Delta_k\|_2 \right| \leq \|\mathbf{g}_{k+1} - \mathbf{g}_k\|_2 \leq \alpha L \|\hat{\Delta}_k\|_2. \quad (19)$$

Recall that R denotes a constant, depending only on the coercivity of $f(x)$, such that $\|x_k - P_*(x_k)\|_2 \leq R$ for all k . This assumption is quite strong, so in Proposition C.7 we provide weaker

sufficient conditions under which this holds. Note that $e_k = F(x_k) - \min F$ is the objective error. Other letters are summarized in table 3. We present the main convergence results in Theorems C.1 and C.2 and proofs and supporting lemmata in

Theorem C.1 (Sublinear convergence). *Suppose that $f(x)$ and $r(x)$ are convex and Assumption 3 is satisfied. If in addition:*

1. **Absolute bound**²: $\|\mathbf{g}_k - \hat{\mathbf{g}}_k\|_2 \leq \varepsilon_{\text{abs}}$, $\alpha < 2/L$ and $\|x_k - P_*(x_k)\|_2 \leq R$ for $k = 1, \dots, K$, then:

$$e_K \leq \max \left\{ \frac{e_0}{K e_0 / (c_7 R^2) + 2}, R \sqrt{c_8 \varepsilon_{\text{abs}}} \right\} \sim \max \left\{ c_7 R^2 \cdot \frac{1}{K}, R \sqrt{c_8 \varepsilon_{\text{abs}}} \right\}.$$

2. **Relative bound**: $r(x) = 0$, $\|\mathbf{g}_k - \hat{\mathbf{g}}_k\|_2 \leq \varepsilon_{\text{rel}} \|\mathbf{g}_k\|_2$, $\alpha < 2/L$ and $\|x_k - P_*(x_k)\|_2 \leq R$ for all k , then:

$$e_k \leq \frac{e_0}{k e_0 / (c_9 R^2) + 1} \sim c_9 R^2 \cdot \frac{1}{k}.$$

The constants c_7 , c_8 and c_9 are defined as in Lemma C.6.

While there exist several results in the literature (see, for example, Theorem 2.2 in [34]) of the same flavor as Part 1 of Theorem C.1, we believe Part 2 to be novel. This is presented as Theorem 2.3 in the main article. We also consider the case where $F(x)$ is non-convex:

Theorem C.2. *Suppose that $F(x)$ satisfies Assumption 3 and $r(x)$ is proximal. Assuming $\|\hat{\mathbf{g}}_k - \mathbf{g}_k\|_2^2 \leq \varepsilon_{\text{abs}}$ for all k , we get:*

$$\begin{aligned} \min_{1 \leq t \leq k} \|\Delta_t\|_2^2 &\leq \frac{c_5}{k+1} e_0 + c_6 \varepsilon_{\text{abs}}, \\ \min_{1 \leq t \leq k} \|\hat{\Delta}_t\|_2^2 &\leq \frac{\hat{c}_5}{k+1} e_0 + \hat{c}_6 \varepsilon_{\text{abs}}, \\ \min_{1 \leq t \leq k} \|\tilde{\Delta}_t\|_2^2 &\leq \frac{\tilde{c}_5}{k+1} e_0 + \tilde{c}_6 \varepsilon_{\text{abs}}. \end{aligned}$$

The constants are defined as in Lemma C.5.

C.1 Supporting lemmas for convergence results

We proceed via a series of Lemmas.

Lemma C.3 (Sequence analysis). *Consider a sequence $e_k \geq 0$ obeying $e_{k+1} \leq e_k - c e_k^2 + d$ for $k = 0, 1, \dots$ where $c > 0$ and $d \geq 0$. We have*

$$e_k \leq \frac{e_0}{e_0 c \cdot k + 2}, \quad k \in \{t : e_0, \dots, e_{t+1} \geq \sqrt{2d/c}\}.$$

In particular, if $d = 0$, then we get

$$e_k \leq \frac{e_0}{e_0 c \cdot k + 1}, \quad k = 0, 1, \dots$$

²We use the symbol “ \sim ” to keep only the leading term in the polynomial.

The first result is a decay of e_k at rate $\sim 1/(ck)$ up until $e_k = \sqrt{2d/c}$. The second result has the rate $\sim 1/(ck)$ for all k .

Proof. Without loss of generality, assume $e_k > 0$ for $k = 0, 1, \dots$. If $e_k \geq \sqrt{2d/c}$, then $e_{k+1} \leq e_k - d$, so $\frac{e_k}{e_{k+1}} \geq 1$. Dividing the condition by $e_{k+1}e_k$ and reorganizing yields

$$\begin{aligned} \frac{1}{e_{k+1}} - \frac{1}{e_k} &\geq \frac{ce_k}{e_{k+1}} - \frac{d}{e_{k+1}e_k} \\ &\geq \begin{cases} c - \frac{d}{2d/c} = \frac{1}{2}c, & d \neq 0, \\ c, & d = 0. \end{cases} \end{aligned}$$

Summing, we obtain $\frac{1}{e_k} \geq \frac{1}{e_0} + \frac{1}{2}kc$ when $d \neq 0$ and $\frac{1}{e_k} \geq \frac{1}{e_0} + kc$ when $d = 0$. Inverting both sides yields the claim. Note that we have assumed that $e_{k+1} \geq \sqrt{2d/c}$ in the $d \neq 0$ case. \square

The next lemma quantifies, under very general assumptions, the amount of descent per iteration of prox-gradient descent we can expect with an inexact gradient estimate.

Lemma C.4. *Suppose that $f(x)$ satisfies Assumption 3 and that $\alpha < 2/L$ if $r(x)$ is convex, while $\alpha < 1/L$ if $r(x)$ is non-convex. Then if $x_{k+1} = x_k - \alpha \hat{\mathbf{g}}_k$:*

$$F(x_{k+1}) \leq F(x_k) - \frac{c_0}{2} \|\alpha \hat{\Delta}_k\|_2^2 + \frac{1}{2c_0} \|\mathbf{g}_k - \hat{\mathbf{g}}_k\|_2^2 \quad (20)$$

$$F(x_{k+1}) \leq F(x_k) - c_1 \|\alpha \Delta_k\|_2^2 + c_2 \|\mathbf{g}_k - \hat{\mathbf{g}}_k\|_2^2 \quad (21)$$

$$F(x_{k+1}) \leq F(x_k) - c_3 \|\alpha \tilde{\Delta}_k\|_2^2 + c_4 \|\mathbf{g}_k - \hat{\mathbf{g}}_k\|_2^2 \quad (22)$$

where $c_0 = \frac{2-1_{\text{ncvx}}-\alpha L}{2\alpha}$, $c_1^{1_{\text{ncvx}}=1} = \frac{1-\alpha L}{4\alpha}$, $c_1^{1_{\text{ncvx}}=0} = \frac{(1-\alpha L)^2+1}{2\alpha^2 L}$, $c_2^{1_{\text{ncvx}}=1} = \frac{\alpha^3 L^2 + \alpha}{2-2\alpha L}$, $c_2^{1_{\text{ncvx}}=0} = \frac{\alpha^2 L}{4}$, $c_3 = (\frac{2}{c_1} + \frac{4\alpha^2 L^2}{c_0})^{-1}$ and $c_4 = c_3(\frac{2c_2}{c_1} + \frac{2\alpha^2 L^2}{c_0^2})$.

Proof. We begin by expanding F .

$$F(x_{k+1}) - F(x_k) = f(x_{k+1}) - f(x_k) + r(x_{k+1}) - r(x_k). \quad (23)$$

When r is convex, we get from the first-order optimality condition of $\mathbf{prox}_{\alpha r}$: $\tilde{\nabla}r(x_{k+1}) = -\hat{\Delta}_k - \alpha \hat{\mathbf{g}}_k$ and, by convexity of r ,

$$r(x_{k+1}) - r(x_k) \leq \langle \tilde{\nabla}r(x_{k+1}), \alpha \hat{\Delta}_k \rangle = -\langle \alpha \hat{\Delta}_k, \hat{\mathbf{g}}_k \rangle - \alpha \|\hat{\Delta}_k\|_2^2.$$

When r is nonconvex, by expanding the definition of $\mathbf{prox}_{\alpha r}$ and comparing the optimal $x = x_{k+1}$ to non-optimal $x = x_k$, we can get

$$r(x_{k+1}) - r(x_k) \leq -\langle \alpha \hat{\Delta}_k, \hat{\mathbf{g}}_k \rangle - \frac{\alpha}{2} \|\hat{\Delta}_k\|_2^2.$$

Note that $\frac{\alpha}{2} < \alpha$ means the last inequality is weaker than the one above it.

Now for $f(x_{k+1}) - f(x_k)$ in (23), apply smoothness of $f(x)$ (Assumption 3) to get:

$$\begin{aligned} f(x_{k+1}) - f(x_k) &\leq \langle \alpha \hat{\Delta}_k, \mathbf{g}_k \rangle + \frac{L}{2} \|\alpha \hat{\Delta}_k\|_2^2 \\ &= \langle \alpha \hat{\Delta}_k, \hat{\mathbf{g}}_k \rangle + \frac{L}{2} \|\alpha \hat{\Delta}_k\|_2^2 + \langle \alpha \hat{\Delta}_k, \mathbf{g}_k - \hat{\mathbf{g}}_k \rangle. \end{aligned}$$

Adding the bounds for $r(x_{k+1}) - r(x_k)$ and $f(x_{k+1}) - f(x_k)$ yields:

$$\begin{aligned}
F(x_{k+1}) - F(x_k) &\leq - \underbrace{\left(\frac{1}{(1 + 1_{\text{ncvx}})\alpha} - \frac{L}{2} \right)}_{c_0} \|\alpha \hat{\Delta}_k\|_2^2 + \langle \alpha \hat{\Delta}_k, \mathbf{g}_k - \hat{\mathbf{g}}_k \rangle \\
&\stackrel{(a)}{\leq} -c_0 \|\alpha \hat{\Delta}_k\|_2^2 + \frac{c_0}{2} \|\alpha \hat{\Delta}_k\|_2^2 + \frac{1}{2c_0} \|\mathbf{g}_k - \hat{\mathbf{g}}_k\|_2^2 = -\frac{c_0}{2} \|\alpha \hat{\Delta}_k\|_2^2 + \frac{1}{2c_0} \|\mathbf{g}_k - \hat{\mathbf{g}}_k\|_2^2
\end{aligned} \tag{24}$$

Where we have used Young's inequality to obtain (a). For the second inequality, we return to (24) and apply $\hat{\Delta}_k = \Delta_k + (\mathbf{g}_k - \hat{\mathbf{g}}_k)$. This yields:

$$\begin{aligned}
F(x_{k+1}) - F(x_k) &\leq -c_0 \|\alpha \Delta_k\|_2^2 + (1 - 2\alpha c_0) \langle \alpha \Delta_k, \mathbf{g}_k - \hat{\mathbf{g}}_k \rangle + (\alpha - \alpha^2 c_0) \|\mathbf{g}_k - \hat{\mathbf{g}}_k\|_2^2 \\
&\stackrel{(a)}{\leq} - \underbrace{\left(c_0 - \frac{(1 - 2\alpha c_0)q}{2} \right)}_{c_1} \|\alpha \Delta_k\|_2^2 + \underbrace{\left(\frac{1 - 2\alpha c_0}{2q} + \alpha - \alpha^2 c_0 \right)}_{c_2} \|\mathbf{g}_k - \hat{\mathbf{g}}_k\|_2^2
\end{aligned}$$

where (a) follows again from Young's inequality, for any $q > 0$. As c_1 and c_2 must be positive, we require $0 < q < \frac{1 - \alpha L}{\alpha^2 L}$ when $1_{\text{ncvx}} = 1$ and $q > \frac{1 - \alpha L}{\alpha^2 L}$ when $1_{\text{ncvx}} = 0$. In particular, we pick $q = \frac{1 - \alpha L}{2\alpha^2 L}$ when $1_{\text{ncvx}} = 1$ and $q = \frac{2 - 2\alpha L}{\alpha^2 L}$ when $1_{\text{ncvx}} = 0$ for this proof.

Finally, observe that:

$$\begin{aligned}
\|\tilde{\Delta}_k\|_2 &\stackrel{(a)}{=} \|\tilde{\nabla} r(x_{k+1}) - \mathbf{g}_{k+1}\|_2 = \|\tilde{\nabla} r(x_{k+1}) - \mathbf{g}_k + \mathbf{g}_k - \mathbf{g}_{k+1}\|_2 \\
&\stackrel{(b)}{\leq} \|\Delta_k\|_2 + \|\mathbf{g}_k - \mathbf{g}_{k+1}\|_2 \stackrel{(c)}{\leq} \|\Delta_k\|_2 + \alpha L \|\hat{\Delta}_k\|_2
\end{aligned}$$

Where (a) follows from the definition of $\tilde{\Delta}_k$, (b) follows from the definition of Δ_k and (c) follows from smoothness of $f(x)$ (Assumption 3). Thus, we have that $\|\tilde{\Delta}_k\|_2^2 \leq 2\|\Delta_k\|_2^2 + 2\alpha^2 L^2 \|\hat{\Delta}_k\|_2^2$. Therefore, combining (20) and (21) yields (22). In particular, $c_3 = (\frac{2}{c_1} + \frac{4\alpha^2 L^2}{c_0})^{-1}$ and $c_4 = c_3(\frac{2c_2}{c_1} + \frac{2\alpha^2 L^2}{c_0^2})$. \square

Note that an immediate consequence of this lemma is the following:

Lemma C.5. *Suppose that $f(x)$ satisfies Assumption 3, that $r(x)$ is proximable and that $\alpha < 2/L$ if $r(x)$ is convex while $\alpha < 1/L$ if $r(x)$ is non-convex. Then:*

$$\begin{aligned}
\sum_{t=0}^k \|\alpha \hat{\Delta}_t\|_2^2 &\leq \hat{c}_5 (F(x_0) - F(x_*)) + \hat{c}_6 \sum_{t=0}^k \|\hat{\mathbf{g}}_t - \mathbf{g}_t\|_2^2 \\
\sum_{t=0}^k \|\alpha \Delta_t\|_2^2 &\leq c_5 (F(x_0) - F(x_*)) + c_6 \sum_{t=0}^k \|\hat{\mathbf{g}}_t - \mathbf{g}_t\|_2^2 \\
\sum_{t=0}^k \|\alpha \tilde{\Delta}_t\|_2^2 &\leq \tilde{c}_5 (F(x_0) - F(x_*)) + \tilde{c}_6 \sum_{t=0}^k \|\hat{\mathbf{g}}_t - \mathbf{g}_t\|_2^2
\end{aligned}$$

for constants $\hat{c}_5 = \frac{2}{c_0}$, $\hat{c}_6 = \frac{1}{c_0^2}$, $c_5 = \frac{1}{c_1}$, $c_6 = \frac{c_2}{c_1}$, $\tilde{c}_5 = \frac{1}{c_3}$ and $\tilde{c}_6 = \frac{c_4}{c_3}$.

Proof. Take the telescopic sums of (20), (21) and (22) respectively. Then, use the fact that by Assumption 3 a minimizer of $F(x)$, namely x_* , exists. Hence $F(x_0) - F(x_k) \leq F(x_0) - F(x_*)$ \square

The next lemma prepares the conditions for us to apply Lemma C.3. Recall that $P_*(\cdot)$ is a projection operator onto the solution set.

Lemma C.6. *Suppose that $F(x)$ is convex and that $f(x)$ satisfies Assumption 3. Then:*

$$e_k^2 \leq c_7 \|x_k - P_*(x_k)\|_2^2 (e_k - e_{k+1}) + c_8 \|x_k - P_*(x_k)\|_2^2 \|\mathbf{g}_k - \hat{\mathbf{g}}_k\|_2^2 \quad (25)$$

for $c_7 = \frac{1}{\alpha^2 c_3}$ and $c_8 = \frac{c_4}{\alpha^2 c_3}$. If, in addition, $r(x) = 0$ and $\|\mathbf{g}_k - \hat{\mathbf{g}}_k\|_2 \leq \varepsilon_{\text{rel}} \|\mathbf{g}_k\|_2$, then

$$e_k^2 \leq c_9 \|x_k - P_*(x_k)\|_2^2 (e_k - e_{k+1}) \quad (26)$$

for $c_9 = \frac{4}{\alpha(2(1-\varepsilon_{\text{rel}}^2) - \alpha L(1+\varepsilon_{\text{rel}}^2))}$.

Proof. By existence of $P_*(x_k)$ and convexity of $F(x)$,

$$\begin{aligned} e_k &= F(x_k) - F(P_*(x_k)) \leq \langle \tilde{\Delta}_k, x_k - P_*(x_k) \rangle \leq \|\tilde{\Delta}_k\|_2 \|x_k - P_*(x_k)\|_2 \\ \Rightarrow e_k^2 &\leq \|\tilde{\Delta}_k\|_2^2 \|x_k - P_*(x_k)\|_2^2 \end{aligned} \quad (27)$$

It remains to bound $\|\tilde{\Delta}_k\|_2^2$. By (22), we get

$$c_3 \alpha^2 \|\tilde{\Delta}_k\|_2^2 \leq e_k - e_{k+1} + c_4 \|\mathbf{g}_k - \hat{\mathbf{g}}_k\|_2^2.$$

Substituting this into (27) yields the first claim.

Now suppose that, in addition, $r(x) = 0$ and $\|\mathbf{g}_k - \hat{\mathbf{g}}_k\|_2 \leq \varepsilon_{\text{rel}} \|\mathbf{g}_k\|_2$. In this case:

$$\begin{aligned} e_k &= f(x_k) - f(P_*(x_k)) \leq \langle \mathbf{g}_k, x_k - P_*(x_k) \rangle \\ &\leq \|\mathbf{g}_k\|_2 \|x_k - P_*(x_k)\|_2 \\ \Rightarrow e_k^2 &\leq \|x_k - P_*(x_k)\|_2^2 \|\mathbf{g}_k\|_2^2. \end{aligned} \quad (28)$$

Using smoothness of $f(x)$, Young's inequality and the bound $\|\mathbf{g}_k - \hat{\mathbf{g}}_k\|_2 \leq \varepsilon_{\text{rel}} \|\mathbf{g}_k\|_2$ we may obtain:

$$\frac{1}{2} (\alpha^2 c_0 - \alpha^2 \varepsilon_{\text{rel}}^2 (c_0 + L)) \|\mathbf{g}_k\|_2^2 \leq e_k - e_{k+1},$$

where $c_0 = \frac{1}{\alpha} - \frac{L}{2}$. (This is equivalent to (21) when $r(x) = 0$). Substituting this into (28) yields the second claim. \square

Proof of Theorem C.1. Rearranging (25) to fit the hypothesis of Lemma C.3 we get:

$$e_{k+1} \leq e_k - \frac{1}{c_7 R^2} e_k^2 + \frac{c_8}{c_7} \varepsilon_{\text{abs}}$$

where we are using the assumption $\|x_k - P_*(x_k)\|_2 \leq R$ as well as the fact that $\|\mathbf{g}_k - \hat{\mathbf{g}}_k\|_2 \leq \varepsilon_{\text{abs}}$. Applying Lemma C.3 yields the Part 1.

Rearranging (26) to fit the hypothesis of Lemma C.3, with $d = 0$, we get:

$$e_k^2 \leq c_9 R^2 (e_k - e_{k+1})$$

where again we have used $\|x_k - P_*(x_k)\|_2 \leq R$. Applying Lemma C.3 again proves Part 2. \square

Proof of Theorem C.2. Follows directly from Lemma C.5. \square

C.2 Boundedness results

In this section, we establish various conditions under which the sequence of iterates, x_k , is bounded. For notational convenience, define $\mathbf{e}_k := \hat{\mathbf{g}}_k - \mathbf{g}_k$.

Proposition C.7. *Assume f is convex. Then there exists an R such that $\|x_k - P_*(x_k)\|_2 \leq R$ for all k under any of the following sets of assumptions:*

1. $r(x) = 0$, $f(x)$ is coercive, $\|\mathbf{e}_k\|_2 \leq \varepsilon_{\text{rel}}\|\mathbf{g}_k\|_2$, $\alpha < 2/L$, and $\varepsilon_{\text{rel}} \leq (2 - L\alpha)/(4 - L\alpha)$.
2. $F(x) = f(x) + r(x)$ is coercive with respect to $\|x\|_2$, $\partial F(x)$ is coercive with respect to $F(x)$ (see Definition 3), $\|\mathbf{e}_k\|_2 \leq \varepsilon_{\text{abs}}$, $F(x)$ satisfies Assumption 3 and $\alpha < 1/L$.

Proof. By the definition of x_{k+1} , we have for $y_k := x_k - \alpha\hat{\mathbf{g}}_k$:

$$r(x) + \frac{1}{2\alpha}\|x - y_k\|_2^2 \geq r(x_{k+1}) + \frac{1}{2\alpha}\|x_{k+1} - y_k\|_2^2$$

for all x . Rearranging it yields

$$r(x) - r(x_{k+1}) + \frac{1}{\alpha}\langle x_{k+1} - y_k, x - x_{k+1} \rangle + \frac{1}{2\alpha}\|x - x_{k+1}\|_2^2 \geq 0, \quad \forall x.$$

When r is convex, we directly have

$$r(x) - r(x_{k+1}) + \frac{1}{\alpha}\langle x_{k+1} - y_k, x - x_{k+1} \rangle \geq 0, \quad \forall x,$$

which follows from the inner-product between $\tilde{\nabla}r(x_{k+1}) + \frac{1}{\alpha}(x_{k+1} - y_k) = 0$ and $x - x_{k+1}$ and applying $r(x) - r(x_{k+1}) \geq \langle \tilde{\nabla}r(x_{k+1}), x - x_{k+1} \rangle$. By defining 1_{ncvx} to be equal to 1 if $r(x)$ is non-convex, and zero otherwise, we may summarize this as:

$$r(x) - r(x_{k+1}) + \frac{1}{\alpha}\langle x_{k+1} - y_k, x - x_{k+1} \rangle + \frac{1_{\text{ncvx}}}{2\alpha}\|x - x_{k+1}\|_2^2 \geq 0, \quad \forall x. \quad (29)$$

On the other hand:

$$\begin{aligned} f(x) - f(x_{k+1}) + \frac{L}{2}\|x_{k+1} - x_k\|_2^2 &= f(x) - f(x_k) + f(x_k) - f(x_{k+1}) + \frac{L}{2}\|x_{k+1} - x_k\|_2^2 \\ &\geq \langle \mathbf{g}_k, x - x_k \rangle + \langle \mathbf{g}_k, x_k - x_{k+1} \rangle = \langle \mathbf{g}_k, x - x_{k+1} \rangle, \end{aligned} \quad (30)$$

where we have used Assumptions 3 and the convexity of $f(x)$. Now adding equations (29) and (30), and using:

$$\frac{1}{\alpha}\langle x_{k+1} - y_k, x - x_{k+1} \rangle - \langle \mathbf{g}_k, x - x_{k+1} \rangle = \frac{1}{\alpha}\langle x_{k+1} - x_k, x - x_{k+1} \rangle + \langle \mathbf{e}_k, x - x_{k+1} \rangle$$

give us

$$\begin{aligned} &F(x) - F(x_{k+1}) + \frac{1}{\alpha}\langle x_{k+1} - x_k, x - x_{k+1} \rangle \\ &+ \frac{L}{2}\|x_{k+1} - x_k\|_2^2 + \langle \mathbf{e}_k, x - x_{k+1} \rangle + \frac{1_{\text{ncvx}}}{2\alpha}\|x - x_{k+1}\|_2^2 \geq 0, \quad \forall x. \end{aligned} \quad (31)$$

In (31), choosing $x = x_k$, $x = P_*(x_0)$, $x = P_*(x_k)$ leads to different analyses. Note that $P_*(x_0)$ and $P_*(x_k)$ are both solutions but may be different.

Part 1: set $x = x_k$ and $r(x) = 0$ Under these assumptions, and recalling that $c_0 := \frac{1}{\alpha} - \frac{1}{L}$, (31) becomes:

$$\begin{aligned} f(x_k) - f(x_{k+1}) &\geq c_0 \|x_{k+1} - x_k\|_2^2 - \langle \mathbf{e}_k, x_k - x_{k+1} \rangle \\ &\geq c_0 \|x_{k+1} - x_k\|_2^2 - \left(\frac{c_0}{2} \|x_{k+1} - x_k\|_2^2 + \frac{1}{2c_0} \|\mathbf{e}_k\|_2^2 \right) \\ &= \frac{c_0}{2} \|x_{k+1} - x_k\|_2^2 - \frac{1}{2c_0} \|\mathbf{e}_k\|_2^2 \end{aligned}$$

where we have used Young's inequality. Under the assumption $\|\mathbf{e}_k\|_2 \leq \varepsilon_{\text{rel}} \|\mathbf{g}_k\|_2$ one can easily show that:

$$\|\mathbf{e}_k\|_2 \leq \frac{\varepsilon_{\text{rel}}}{1 - \varepsilon_{\text{rel}}} \|\hat{\mathbf{g}}_k\|_2 = \frac{\varepsilon_{\text{rel}}}{1 - \varepsilon_{\text{rel}}} \|x_{k+1} - x_k\|_2.$$

and hence:

$$\begin{aligned} f(x_k) - f(x_{k+1}) &\geq \frac{c_0}{2} \|x_{k+1} - x_k\|_2^2 - \frac{1}{2c_0} \frac{\varepsilon_{\text{rel}}^2}{(1 - \varepsilon_{\text{rel}})^2} \|x_{k+1} - x_k\|_2^2 \\ &= \left(\frac{c_0}{2} - \frac{\varepsilon_{\text{rel}}^2}{2\alpha^2 c_0 (1 - \varepsilon_{\text{rel}})^2} \right) \|x_k - x_{k+1}\|_2^2 \end{aligned}$$

Recalling that $c_0 = \frac{1}{\alpha} - \frac{1}{L}$ we see that for $\alpha < 2/L$ and $\varepsilon_{\text{rel}} \leq (2 - L\alpha)/(4 - L\alpha)$ the sequence $\{f(x_k)\}$ is monotonically decreasing. By coercivity, there exists an R such that $\|x_k - \mathbf{P}_*(x_k)\|_2 \leq R$ for all k .

Part 2. From (22) we have that:

$$F(x_{k+1}) - F(x_k) \leq -c_3 \alpha^2 \|\tilde{\Delta}_k\|_2^2 + c_4 \|\mathbf{e}_k\|_2^2 \leq -c_3 \alpha^2 \|\tilde{\Delta}_k\|_2^2 + c_4 \varepsilon_{\text{abs}}^2 \quad (32)$$

where we are also using the assumption $\|\mathbf{e}_k\|_2 \leq \varepsilon_{\text{abs}}$. By definition, $-\tilde{\Delta}_k \in \partial F(x_{k+1})$ and hence by coercivity of ∂F with respect to F , there exists an R_1 such that $F(x_{k+1}) > R_1$ implies that $\|\tilde{\Delta}_k\|_2^2 > \frac{c_4 \varepsilon_{\text{abs}}^2}{c_3 \alpha^2}$. This in turn implies that the right-hand side of (32) is strictly negative. Therefore, by induction, $F(x_k) \leq \max\{F(x_0), R_1\}$ for all $k \geq 0$. Finally, by coercivity of $F(x)$ with respect to $\|x\|_2$ and the fact that $\{F(x_k)\}_{k=0}^\infty$ is bounded, $\{\|x_k\|_2\}_{k=1}^\infty$ is bounded. It then follows that $\{\|x_k - \mathbf{P}_*(x_k)\|_2\}_{k=1}^\infty$ is bounded. \square

D Proofs for Section 3

Proof of Theorem 3.1. By assumption, we may choose ε_{rel} and n satisfying:

$$\psi + \rho^n < \varepsilon_{\text{rel}} < \frac{1 - \alpha L}{2 - \alpha L}$$

hence by Theorem 2.1, $\|\mathbf{g}_k - \hat{\mathbf{g}}_k\|_2 \leq \varepsilon_{\text{rel}} \|\mathbf{g}_k\|_2$ for all k . Since in addition $\varepsilon_{\text{rel}} \leq (2 - \alpha L)/(4 - \alpha L)$, from Proposition C.7, $\|x_k - \mathbf{P}_*(x_k)\|_2 \leq R$ for some fixed R . The stated convergence rate then follows from Theorem C.1. \square

Proof of Theorem 3.2. From Theorem 2.2, we get that $\|\mathbf{g}_k - \hat{\mathbf{g}}_k\|_2 \leq 2^{3/2}\sqrt{\tau\sigma H}$ for all $k = 1, \dots, K$ with probability $1 - (s/d)^{b_2 s}$. The claim follows by combining this with Theorem C.1. Note that $\|x_k - P_*(x_k)\|_2 \leq R$ for all k by Proposition C.7 part 2. \square

Proof of Theorem 3.3. This follows from Theorem C.2 Part 2 with $\varepsilon_{\text{abs}} = 2\sqrt{2\tau\sigma H}$, which is guaranteed by Theorem 2.2. \square

E More Numerical Results

E.1 Synthetic example

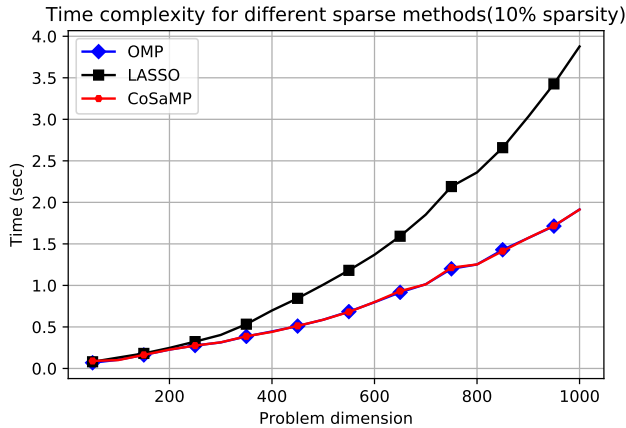


Figure 5: Running time *v.s.* problem dimension for different sparse methods when the sparsity ratio is fixed.

We investigate the runtime of ZORO with different sparse gradient estimators (*i.e.*, estimating the sparse gradients with OMP, LASSO or CoSaMP). The experiments are executed in MATLAB R2019a on a Windows 10 laptop with Intel i7-8750H CPU (6 cores at 2.2GHz) and 32GB of RAM. We implement all three versions of ZORO by ourselves. In particular, for the LASSO based gradient estimator, we use FISTA to be solver, and choose the regularizing parameter λ_{k+1} at $(k + 1)$ -th iteration by the ratio of the ℓ_2 residual squared and ℓ_1 -norm from the last iteration: $\lambda_{k+1} = c\|\mathbf{y}_k - Z_k\hat{\mathbf{g}}_k\|_2^2/\|\hat{\mathbf{g}}_k\|_1$, where c is a fixed parameter throughout all iterations. Furthermore, the stop criteria of all three gradient estimators are set to $\|x_{k+1} - x_k\|_2/\|x_k\|_2 \leq 10^{-6}$.

We consider the problem of minimizing a quadratic function $f(x) = x^\top Ax/2$, where $A \in \mathbb{R}^{d \times d}$ is a diagonal matrix with s non-zero randomly generated positive elements. The runtime is evaluated with varying problem dimension (see Figure 5) and sparsity level (see Figure 6). Moreover, the runtimes reported in Figures 5 and 6 are based on 30 iterations of gradient descent, and averaged over 10 random tests. We find that the greedy methods, CoSaMP and OMP, have a speed advantage when the problem dimension is large and sparsity level is small, while the LASSO solver is fastest when both d and s are small. We emphasize that the gradients estimated by all three methods offer almost identical convergence performance on these easier synthetic tasks, so the stopping criterion of ZORO will not affect our observations.

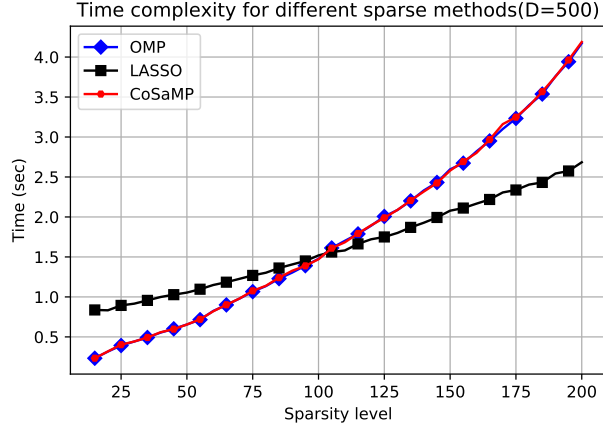


Figure 6: Running time *v.s.* sparsity level for different sparse methods when the the problem dimension is fixed.

E.2 Sparse adversarial attack on ImageNet

For this numerical experiment, we use the code from <https://github.com/KaidiXu/ZO-AdaMM> with a few modifications. We focus on the per-image untargeted attack scenario. For the objective function, we change the ℓ_2 -norm of distortion to ℓ_0 -norm. At each iteration, we randomly select a subspace of 2000 variables and generate 50 random Rademacher perturbation signals in this subspace. We use a much larger step-size than [29] since our gradient estimate has much better precision. Note that there are several hyper-parameters (step-size, decay parameter, subspace dimension, ZORO parameters, etc.) that have not been fully optimized. We plan to address this issue along with more diverse simulation settings (targeted attacks, universal attacks, etc.) in a future work. Some pictures of successful sparse attacks by ZORO are presented in Figure 4, and we further provide an enlarge version in Figure 7 for a clearer view.

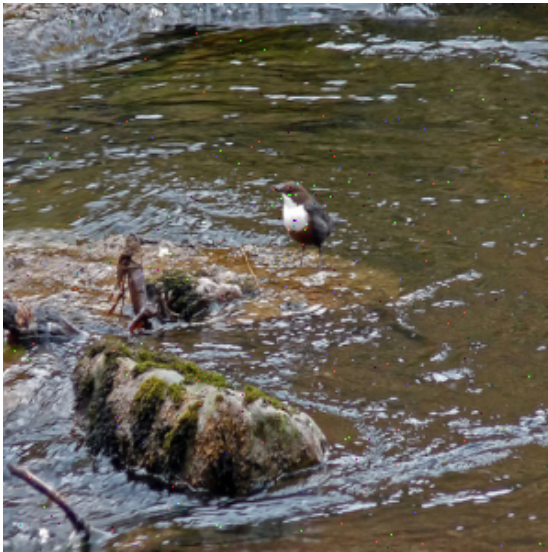
Notice that the distortions are similar with impulse noise, which can be mitigated by a median filter. We use the tool `ndimage.median_filter` from `scipy`. We use \mathcal{A} to denote the set of adversarial images (original image+distortion) that are successfully attacked by ZORO. We use \mathcal{I}_1 to denote the set of image IDs that are not recovered. The ratio of images in \mathcal{A} been identified to the true label after filtering is the recover successful rate: $1 - |\mathcal{I}_1|/|\mathcal{A}|$. We then analyze the side-effect of median filter by apply it to the original images of \mathcal{A} . We use \mathcal{I}_2 to denote the set of image IDs that are mis-classified. The distortion rate is the ratio of images been assigned an incorrect label: $|\mathcal{I}_2|/|\mathcal{A}|$. We summarize the images indexes from these two experiments and calculate the total accuracy reduction: $|\mathcal{I}_1 \cup \mathcal{I}_2|/|\mathcal{A}|$. Note that there are some overlapping IDs in \mathcal{I}_1 and \mathcal{I}_2 .



(a) “corn” → “ear, spike, capitulum”



(b) “plastic bag” → “shower cap”



(c) “water ouzel, dipper” → “otter”



(d) “thimble” → “measuring cup”

Figure 7: Examples of adversarial images, true labels, and mis-classified labels. These pictures are same as in Figure 4, but enlarged.